

# Analyzing cross-talk between superimposed signals: Vector norm dependent hidden Markov models and applications

Laura Julia Vanegas<sup>\*†</sup>, Benjamin Eltzner<sup>\*†</sup>, Daniel Rudolf<sup>\*†</sup>,  
Miroslav Dura<sup>‡</sup>, Stephan E. Lehnart<sup>‡§</sup>, and Axel Munk<sup>\*¶</sup>

December 23, 2024

## Abstract

We propose and investigate a hidden Markov model (HMM) for the analysis of aggregated, super-imposed two-state signal recordings. A major motivation for this work is that often these recordings cannot be observed individually but only their superposition. Among others, such models are in high demand for the understanding of cross-talk between ion channels, where each single channel might take two different states which cannot be measured separately. As an essential building block we introduce a parametrized vector norm dependent Markov chain model and characterize it in terms of permutation invariance as well as conditional independence. This leads to a hidden Markov chain “sum” process which can be used for analyzing aggregated two-state signal observations within a HMM. Additionally, we show that the model parameters of the vector norm dependent Markov chain are uniquely determined by the parameters of the “sum” process and are therefore identifiable. Finally, we provide algorithms to estimate the parameters and apply our methodology to real-world ion channel data measurements, where we show competitive gating.

**Keywords:** Hidden Markov models, vector norm dependency, permutation invariance, lumping property, aggregated data, cross-talk, ion channels

---

<sup>\*</sup>Institute for Mathematical Stochastics, Georg-August-Universität Göttingen, Germany

<sup>†</sup>The authors contributed equally.

<sup>‡</sup>Cellular Biophysics and Translational Cardiology Section, Heart Research Center Göttingen, Department of Cardiology & Pneumology, University Medical Center Göttingen, Germany

<sup>§</sup>DZHK (German Centre for Cardiovascular Research), partner site Göttingen, Germany

<sup>¶</sup>Felix-Bernstein-Institute for Mathematical Statistics, Göttingen, Germany

‡Corresponding author, e-mail: munk@math.uni-goettingen.de

# 1 Introduction

*Hidden Markov models* (HMMs) have a long history, see (Cappé et al., 2005; Westhead and Vijayabaskar, 2017; Zucchini et al., 2017) for recent monographs, and are nowadays well established tools to model signals that stem from an underlying, not directly observable Markov chain. Whereas classical theory is mainly concerned with univariate scenarios, more recently, much progress has been made in the case where the Markov chain is multivariate and exhibits dependencies between its components. Such models have been proven useful when analyzing smartphone sensor data of many sources (van der Kamp and Osgood, 2017), disease interaction in medical research (Sherlock et al., 2013), or for classification tasks in computer vision (Brand et al., 1997) to mention a few applications. An asymptotic analysis of multivariate HMMs can be found, e.g., in (Bielecki et al., 2013) and computational aspects are discussed in (Touloupou et al., 2020). However, only little methodology is available for the case when the signal can not be marginally observed but only a superimposed version is available. This appears somewhat surprising, as the modeling, recovery and analysis of superimposed Markovian signals is in high demand for various applications, e.g., ion channel investigations (Chung et al., 2007), super-resolution microscopy (Staudt et al., 2020), or magnetotelluric data assessment (Neukirch et al., 2019). We refer to Section 1.5 for a more comprehensive account. Besides the masking effect from superposition, such analysis is hindered by “crosstalk” between these signals, i.e., by its statistical dependency. Moreover, in many applications the understanding of this “crosstalk” is actually one of the primary aims of the data analysis. Therefore, in this paper we develop and characterize a novel Markov chain model allowing crosstalk between single two-state signals as well as employing it in a HMM and provide statistical methodology for its analysis. While our methodology is applicable in any situation where superpositions of general two-state Markov-systems are observed we focus for illustrative purposes on a challenging ion channel application and show the advantages of our approach in that scenario.

## 1.1 Ion channels ensembles

Ion channels are large protein complexes in the cell membranes of living organisms that control the flux of charged ions into and out of the cell. Ion concentrations in cells are crucial for key functionality of cells like signal transmission in nerve cells and contraction of muscle cells (Chung et al., 2007). Therefore, understanding the conductance properties of ion channels is a major endeavor in physiology and of great medical importance. Fundamental to this is the patch-clamp technique which allows to measure ion channel conductivity of single channels and the development of artificial lipid bilayers has facilitated the exclusion of interfering environmental factors, see (Sakmann and Neher, 1995). In addition, current investigation of automatized patch-clamp-like techniques can lead to faster data collection, see (Perkel, 2010). Single channel modeling is often done via HMMs, see e.g. (Sakmann and Neher, 1995; Ball and Rice, 1992; Becker et al., 1994; de Gunst et al., 2001; Venkataramanan and Sigworth, 2002; Khan et al., 2005). More recently, also non-

parametric change point regression methods have been developed as a flexible and computationally efficient alternative, see e.g. (Gnanasambandam et al., 2017; Pein et al., 2018)

However, isolating experimentally a single ion channel is not always possible or desirable. Measuring conductivity of multiple ion channels simultaneously allows to simplify experimental design and enables the study of channel interactions. Moreover, having a reliable model for multiple channels can lead to biological insight as observed in (Mirams et al., 2011). The recently developed non-parametric change point regression methods for single channel analysis, while versatile and powerful data analysis tools, do not provide enough structure to infer properties of single channels from total conductivity of an ensemble of channels.

In contrast, we will see that HMMs allow enough structure to recover channel dependencies from superpositions by encoding interactions in the transition matrices. The simplest case occurs for independent channels (Dabrowski and McDonald, 1992), which, however, is not fulfilled in many applications, see, e.g., (Keleshian et al., 2000) and Section 1.4. For recovering the dependency from superpositions when the channels interact the state of the art model and method was developed by Chung and Kennedy (1996). However, this relies on a simplifying assumption that may be very restrictive for application purposes, allowing only “cooperative” dependency, i.e., a higher probability for the channels to be in the same state. In this paper, we develop a model that is, on the one hand, sufficiently flexible to describe a wide range of behaviors, with assumptions that fit well to the application. On the other hand, it is specific enough to allow for estimation of the parameters from superimposed data. In Section 1.4 and Section 4, we show a competitive dependency for ion channels which play an important role in cardiac muscle cells, i.e., there is a higher probability for the channels to be in opposite states, where previously known methods do not provide a good fit.

## 1.2 Setup and main contributions

Suppose there are  $\ell \in \mathbb{N}$  *emitters* (single ion channels), where each generates a  $\{0, 1\}$ -valued discrete-time sequence which we call *signal*. The two values  $\{0, 1\}$  ( $0 \hat{=}$  closed,  $1 \hat{=}$  open) that each entry of the sequence can attain are called *states*. Each signal at each time-point is absorbed by an aggregation procedure, leading to a superposition of the whole system of signals, which is afterwards noisily recorded by the receiver. For ion channels, this corresponds to the measurement of total current of the superimposed channels. For a schematic view of this setting see Figure 1. We motivate our model in the setting of our main application, the understanding of ensemble ion channel behavior, and provide interpretations in that scenario. There, a single ion channel takes the role of an emitter and their conductance takes the role of the signals.

Suppose that all random variables are defined on a common probability space  $(\Omega, \mathcal{F}, \mathbb{P})$ . As an essential building block, for any  $\ell \in \mathbb{N}$ ,  $k \in \mathbb{N}$  and  $j \in \{1, \dots, \ell\}$  let  $X_k^{(j)}: \Omega \rightarrow \{0, 1\}$  be a random variable describing the state of the  $j$ -th emitter at time point  $k$ . Considering those random variables simultaneously in  $k$  we assume

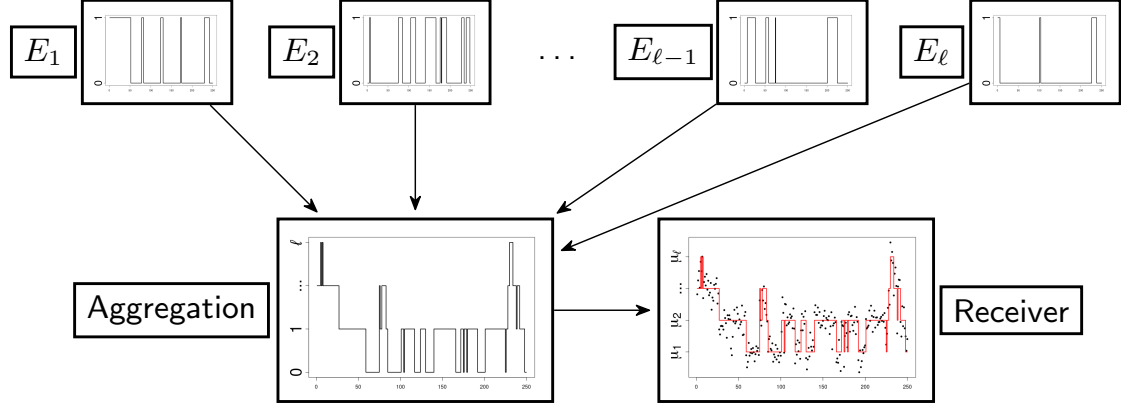


Figure 1: At a fixed time-point each emitter produces a  $\{0, 1\}$ -valued entry of the signal. The experimental setup now leads to an aggregation, where the signals are superposed. Such aggregation is not directly observable but is hidden according to an HMM, such that only the sum of all signals, perturbed by random noise, can be recorded.

that each of the  $\ell$  individual signals from the emitters is modeled by a homogeneous Markov chain  $(X_k^{(j)})_{k \in \mathbb{N}_0}$ , with  $j = 1, \dots, \ell$  on the finite state space  $\{0, 1\}$ . Then, the whole system of the  $\ell$  signals (or emitters) can be modeled by an  $\ell$ -dimensional homogeneous Markov chain  $(X_k)_{k \in \mathbb{N}_0}$  on the finite state space  $\{0, 1\}^\ell$ , where  $X_k := (X_k^{(1)}, \dots, X_k^{(\ell)})^T$ . Note that the transition matrix, say  $M \in \mathbb{R}^{2^\ell \times 2^\ell}$ , of the multidimensional process contains the full information on the dependence (coupling) between emitters. Therefore, finding suitable parametrizations of the matrix  $M$  is one of the key points of this paper.

Most relevant to this paper is that we have (noisy) measurements only on the sum of the system of signals of the individual emitters and not for each emitter separately, i.e., marginally. Therefore, we are interested in the “sum” process  $(S_k)_{k \in \mathbb{N}}$  on the finite state space  $[\ell] := \{0, \dots, \ell\}$  given by

$$S_k := \sum_{j=1}^{\ell} X_k^{(j)}.$$

Note that the sequence of random variables starts with  $S_1$  to restrict the influence of the initial distribution of  $(X_k)_{k \in \mathbb{N}_0}$ . The process  $(S_k)_{k \in \mathbb{N}}$  can be seen as counting how many emitters are in state “1” (i.e., how many channels are open in the case of ion channels) at each discretized time point  $k \in \mathbb{N}$ . Observe that from a path of  $(S_k)_{k \in \mathbb{N}}$  it is generally not possible to recover the individual paths of  $(X_k)_{k \in \mathbb{N}_0}$ . Even worse, the process  $(S_k)_{k \in \mathbb{N}}$  is not necessarily a Markov chain.

However, if the vector Markov chain  $(X_k)_{k \in \mathbb{N}_0}$  satisfies the so-called lumping property, see Definition 2.1 below and also (Kemeny and Snell, 1976, Section 6.3), then the corresponding “sum” process is indeed a Markov chain. This is a desirable property, since if it is satisfied we can use standard techniques to estimate the transition matrix of the sum process. Moreover, the transition matrix of  $(X_k)_{k \in \mathbb{N}_0}$

determines completely the one of  $(S_k)_{k \in \mathbb{N}}$ , see Theorem 2.4 below.

A major aim of our paper is to characterize those situations which allow to recover information of the transition matrix  $M$  of the vector Markov chain  $(X_k)_{k \in \mathbb{N}_0}$  knowing only the behavior of  $(S_k)_{k \in \mathbb{N}_0}$ . In the application to ion channels, this can be translated as obtaining information of individual channel dynamics and their interactions by knowing the number of open channels at each time.

As a fundamental model for the paper we introduce a *vector norm dependent* (VND) Markov chain model which satisfies both desirable properties and allows a reasonable interpretation in applications, in particular, the ion channel data analysis setting.

**Definition 1.1** (Vector Norm Dependency). A vector Markov chain  $(X_k)_{k \in \mathbb{N}_0}$  on  $\{0, 1\}^\ell$  with transition matrix  $M^{(\text{VND})} = (m_{x,y}^{(\text{VND})})_{x,y \in \{0,1\}^\ell}$  is called vector norm dependent (VND) if for all  $i \in \{1, \dots, \ell\}$ ,  $r \in [\ell]$ ,  $k \in \mathbb{N}_0$  and  $b \in \{0, 1\}$ , the expression

$$\mathbb{P} \left( X_{k+1}^{(i)} = b \mid X_k^{(i)} = b, \|X_k\|_1 = r \right) \quad (1)$$

is independent of  $i$  and  $k$  and

$$m_{x,y}^{(\text{VND})} = \prod_{i=1}^{\ell} \mathbb{P} \left( X_{k+1}^{(i)} = y^{(i)} \mid X_k^{(i)} = x^{(i)}, \|X_k\|_1 = \|x\|_1 \right), \quad (2)$$

for any  $x = (x^{(1)}, \dots, x^{(\ell)})^T$  and  $y = (y^{(1)}, \dots, y^{(\ell)})^T$  with  $x, y \in \{0, 1\}^\ell$ .

Observe that within the VND Markov chain model the transition matrix  $M^{(\text{VND})}$  is determined by  $2\ell$  parameters,  $\lambda_j$  and  $\eta_{j+1}$ ,  $j = 0, \dots, \ell - 1$  which are given by

$$\lambda_j := \mathbb{P} \left( X_{k+1}^{(i)} = 0 \mid X_k^{(i)} = 0, \|X_k\|_1 = j \right), \quad (3)$$

$$\eta_{j+1} := \mathbb{P} \left( X_{k+1}^{(i)} = 1 \mid X_k^{(i)} = 1, \|X_k\|_1 = j + 1 \right). \quad (4)$$

These parameters have a direct interpretation, as the probability of each emitter to stay in state “0” or “1” given the previous value of the emitter and the total number of emitters in state “1”. With this we are in the position to discuss our main theoretical results.

**Main theoretical contributions.** We show that the VND Markov chain model with corresponding transition matrix  $M^{(\text{VND})}$  satisfies that:

1. The corresponding “sum” process  $(S_k)_{k \in \mathbb{N}}$  is again a Markov chain,
2. we can retrieve  $M^{(\text{VND})}$  from  $(S_k)_{k \in \mathbb{N}}$  (using (12) from below), see Theorem 1.5.

In order to make the VND Markov chain model applicable for practical purposes, it is helpful to have a more detailed understanding of this property and simple conditions how to validate it. To this end, we introduce two more properties, interpret them in terms of the ion channel scenario and show how they relate to vector norm dependency. The first one is as follows:

**Definition 1.2** (Permutation invariance). We call a vector Markov chain  $(X_k)_{k \in \mathbb{N}_0}$  *permutation invariant* if for any  $k \in \mathbb{N}$ ,  $x, y \in \{0, 1\}^\ell$ , and any permutation matrix  $P \in \{0, 1\}^{\ell \times \ell}$  holds

$$\mathbb{P}(X_{k+1} = y \mid X_k = x) = \mathbb{P}(X_{k+1} = Py \mid X_k = Px).$$

This condition makes sense in our illustrative application, since it is reasonable to assume that there is no “leading” channel, but all channels have the same transition mechanism and every channel interacts with every other channel according to the same dynamics. This condition constrains cooperative gating in particular, since any interaction must have the same effect on all channels, which only allows for cooperative gating among all channels, not subsets of them. It also turns out that this property implies that the sum of the individual channel currents, i.e., the “sum” process  $(S_k)_{k \in \mathbb{N}}$ , is again a Markov chain. This formerly described desirable feature is proved by using the well known concept of the lumping property, see Sections 2.1 and 2.2.

Now we turn to the second property:

**Definition 1.3** (Conditional independence). We call  $(X_k)_{k \in \mathbb{N}_0}$  *conditionally independent* (w.r.t. the past), if

$$\mathbb{P}(X_{k+1} = y \mid X_k = x) = \prod_{i=1}^{\ell} \mathbb{P}(X_{k+1}^{(i)} = y^{(i)} \mid X_k = x),$$

for any  $k \in \mathbb{N}_0$  and for all  $x, y \in \{0, 1\}^\ell$  where  $y = (y^{(1)}, \dots, y^{(\ell)})^T$ .

In our application, this condition translates to saying that, given the state at the previous time point, all channels behave statistically independent. A dependency between channels is therefore only possible through the state at the previous time point, so interaction between channels always occurs with temporal delay.

Now we can state our main result on the characterization of a VND Markov chain model.

**Theorem 1.4** (Characterization of VND Markov chain). *For a vector Markov chain  $(X_k)_{k \in \mathbb{N}_0}$  assume that the initial distribution is permutation invariant<sup>1</sup>. Then, the following statements are equivalent:*

1. *The Markov chain  $(X_k)_{k \in \mathbb{N}_0}$  is vector norm dependent;*
2. *The Markov chain  $(X_k)_{k \in \mathbb{N}_0}$  is permutation invariant and conditional independent.*

This result provides a justification of the VND Markov chain model for many ion channel recordings, since permutation invariance and conditional independence allow for a clear interpretation within this setting. As a side effect we obtain from

---

<sup>1</sup>The distribution of  $X_0$  is permutation invariant if  $\mathbb{P}(X_0 = y) = \mathbb{P}(X_0 = Py)$  for any  $y \in \{0, 1\}^\ell$  and any permutation matrix  $P \in \{0, 1\}^{\ell \times \ell}$ .

the permutation invariance of a VND Markov chain that the “sum” process  $(S_k)_{k \in \mathbb{N}}$  is indeed a Markov chain. In the following we denote the transition matrix of this Markov chain by  $Q^{(\text{VND})} \in \mathbb{R}^{(\ell+1) \times (\ell+1)}$ .

The transition matrix  $Q^{(\text{VND})}$  can be explicitly stated in terms of the parameters  $\lambda_j$  and  $\eta_{j+1}$  for  $j = 0, \dots, \ell - 1$  of the VND Markov chain, see Proposition 2.19. By equation (12), see below, also  $M^{(\text{VND})}$  can be explicitly stated in terms of the parameters  $\lambda_j$  and  $\eta_{j+1}$ . This enables one to extract knowledge about  $M^{(\text{VND})}$  from  $Q^{(\text{VND})}$ . More surprisingly, the “sum” process determines the parameters of  $M^{(\text{VND})}$  uniquely:

**Theorem 1.5** (Inverse lumping identifiability for VND Markov chains). *Let  $(S_k)_{k \in \mathbb{N}}$  be a “sum” Markov chain with transition matrix  $Q^{(\text{VND})}$  on  $[\ell]$  based on a vector norm dependent Markov chain  $(X_k)_{k \in \mathbb{N}_0}$  with transition matrix  $M^{(\text{VND})}$ . If  $\ell$  is odd, then the parameters  $\lambda_j$  and  $\eta_{j+1}$  with  $j = 0, \dots, \ell - 1$  defining  $M^{(\text{VND})}$  are uniquely determined by the entries of  $Q^{(\text{VND})}$ . If  $\ell$  is even, the same holds true provided that  $\lambda_{\ell/2} \geq 1 - \eta_{\ell/2}$ .*

Let us emphasize that the VND modeling is flexible enough for describing the system behavior we are interested in and at the same time is specific enough so that we can recover the parameters uniquely from the transition matrix  $Q^{(\text{VND})}$ . This conclusion cannot be reached by the lumping property or even permutation invariance alone, since the number of free parameters of  $M$  is larger than the number of entries of  $Q$  (see Remarks 2.5 and 2.11), which leads to an underdetermined system.

### 1.3 Estimation in the hidden VND Markov model and software

Suppose a VND Markov chain model with corresponding Markov chain “sum” process  $(S_k)_{k \in \mathbb{N}}$  is given. Then, we model the aggregated recordings with a HMM  $(S_k, Y_k)_{k \in \mathbb{N}}$  where  $(S_k)_{k \in \mathbb{N}}$  is the hidden Markov chain and  $(Y_k)_{k \in \mathbb{N}}$  is the observed sequence. An important scenario, see Example 3.1 below, is the following: For a standard normally distributed real-valued random variable  $\xi$  and  $(\mu, \nu, \sigma_0, \dots, \sigma_\ell) \in \mathbb{R}^2 \times (0, \infty)^{\ell+1}$  the  $Y_k$ s depend on the *number* of open channels, i.e., the value of  $S_k$ , through

$$Y_k = \mu + S_k \nu + \sigma_{S_k} \xi, \quad k = 1, \dots, K.$$

By the VND property of the vector Markov chain model we have that  $(S_k)_{k \in \mathbb{N}_0}$  is a Markov chain and therefore we can in principle estimate the corresponding transition matrix  $Q^{(\text{VND})} \in \mathbb{R}^{(\ell+1) \times (\ell+1)}$  with the Baum-Welch algorithm (EM-algorithm) as introduced in Baum et al. (1970). However, standard implementations of the Baum-Welch algorithm do not allow for using a specific parametric model for the transition matrix of the hidden Markov chain, so we apply a customized algorithm to achieve this (see Section 3). Since the parametrization of  $Q^{(\text{VND})}$  makes it hard to derive a closed form for the maximization step we optimize it numerically.

We finally mention, that our customized Baum-Welch algorithm is designed to maximize the likelihood of the HMM, and therefore it also can be applied to the

Chung and Kennedy (1996)-model and it achieves a better estimation accuracy than the least-squares procedure proposed there.

The implementation of an R package for simulation and estimation in the VND model can be found at <https://github.com/ljvanegas/VND>.

## 1.4 Application to ion channel data

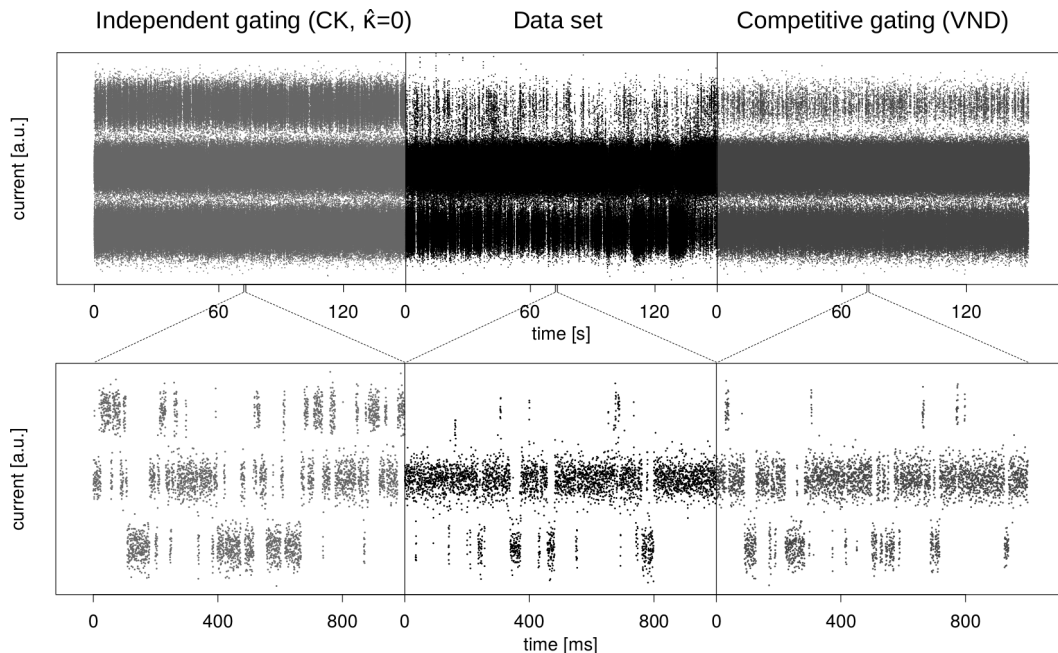


Figure 2: A current measurement on multiple channels in a synthetic lipid bilayer is compared to simulated data from two models. The data is displayed in the middle, a simulated trace from the Chung-Kennedy model using the estimated parameter value  $\hat{\kappa} = 0$ , which amounts to independent channels, is displayed to the left and a simulated trace from the VND model with competitive gating is displayed on the right. The parameters used for the simulations are the estimated parameters from the data under the respective models. The full data exhibit structure on long time scales which cannot be reproduced by either model and, due to signal filtering, more intermediate values between the levels are measured. However, it is obvious, especially from the zoom-in plots in the lower panel, that the competitive gating VND model reflects the channel gating behavior much more faithfully than the CK model predicting uncoupled channels.

In Section 4, we apply this framework to a time series of current measurements on a synthetic lipid bilayer with multiple RyR2 ion channels. In the present experiment, the  $\text{Ca}^{2+}$  concentration on the cis side is low, namely 150 nM, while the concentration on the trans side is very high, namely 5 mM and 10 mM, respectively. Data were provided by the Lehnart Lab of the Cellular Biophysics and Translational Cardiology Section in the Heart Research Center Göttingen (HRCG). We compare with the only competing model that is widely used in the literature,



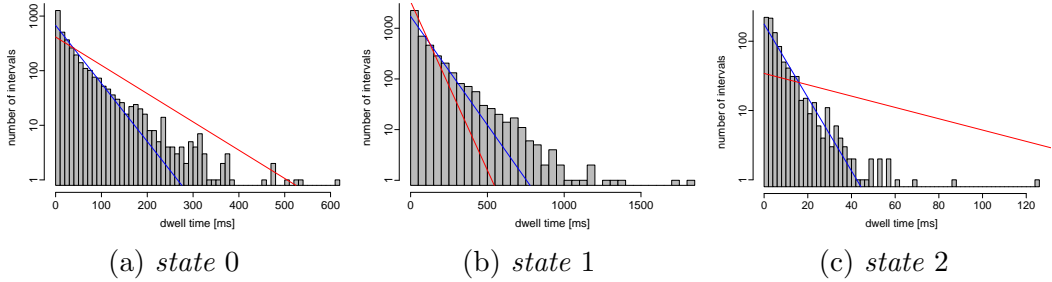


Figure 3: *Dwell times in the three states compared with model predictions. The blue line indicates the prediction from the estimated parameters of the VND model, the red curve corresponds to the estimate by the CK model. The histograms display dwell times extracted from the Viterbi path. Note that the vertical axis is logarithmic, which means that the excess of long dwell times over model predictions is less pronounced than it appears. One can clearly see that the predictions of the VND model fit the data much better than the predictions of the CK model.*

namely the Chung-Kennedy model (Chung and Kennedy, 1996). In contrast to the VND model, the Chung-Kennedy transition matrix  $M^{(\text{CK})}$  of  $(X_k)_{k \in \mathbb{N}_0}$  is given by

$$M^{(\text{CK})} = \kappa M^{(\text{FC})} + (1 - \kappa) M^{(\text{UC})},$$

where  $\kappa \in [0, 1]$  is a mixing parameter between the fully coupled case ( $M^{(\text{FC})}$ ) and the fully uncoupled case ( $M^{(\text{UC})}$ ); more details are given in Section 2.2. We find that our model achieves a significantly better fit, as illustrated in Figures 2, 3 and Figure 5 in Supplement A. Our model can detect that “competitive gating” occurs, meaning that the system prefers only one channel to be open, while the other (or others) are closed and the channels effectively compete for the role of being the single open channel. This surprising behavior has not been observed for RyR2 channels to date, because previously used models could not identify competitive gating and most experiments have focused on varying  $\text{Ca}^{2+}$  concentration on the cis side.

The VND model has limited power when trying to determine the true number of channels, which was determined as roughly  $\ell \approx 20$  at the end of the experiment by adding a high concentration of calcium on the cis side, because throughout the measurement time the highest number of open channels at any given time is two. However, we show that the vector norm dependent model is fairly robust to underestimating the number of channels. In that case, it tends to slightly underestimate competitive gating, which means in turn that if estimated parameters in the vector norm dependent model indicate competitive gating, this finding is robust even if the number of channels was underestimated.

## 1.5 Related work

Since the introduction of HMMs in the late 1960s (Baum and Petrie, 1966; Baum et al., 1970), they provide a widely used machinery for a variety of problems in

biology (Krogh et al., 2001; Chen et al., 2016) and medicine (Manogaran et al., 2018), among many other areas of application. In particular, HMMs are established as a standard modeling tool for ion channels for decades, see e.g. (Ball and Rice, 1992; Becker et al., 1994; Venkataramanan and Sigworth, 2002; Khan et al., 2005).

Various extensions of HMMs have been introduced, see e.g. (Sin and Kim, 1995; Mari et al., 1997; Fine et al., 1998; Guan et al., 2016; Siekmann et al., 2016; Diehn et al., 2019). Most related to our setting are factorial HMMs (Ghahramani and Jordan, 1997; Chen et al., 2009), that consider several independent unobservable chains. In this sense, each individual channel can be seen as an unobservable layer. In contrast, in our setting the dependency structure plays a key role. Coupled HMMs, see (Brand et al., 1997), deal with dependency by embedding the system in a multidimensional chain (as we do), and then applying HMM techniques to it. However, in our setting we can not observe the state of each individual channel at any moment in time, which significantly complicates the situation and is the major motivation for our approach.

There are several works related to this situation, i.e., when the observations depend only on the sum of Markov chains, most of them require independence of channels (see e.g. Yeo et al. (1989); Fredkin and Rice (1991); Dabrowski and McDonald (1992); Klein et al. (1997)). The concept of exchangeability of Markov chains in a multidimensional setting, which is equivalent to permutation invariance, was explored by Gottschau (1992). For continuous time Markov chains the concept of such “aggregations” was developed by Ball et al. (1997). Most related to our work is the Chung-Kennedy model proposed by Chung and Kennedy (1996), which is a simple model of dependency of channels. However, the dependency structure of such a model is limited since it is a linear interpolation between the fully coupled case (where all channels are equal) and the independent case. In particular, it can only model “positive cooperative gating”, where all channels have a tendency to open and close synchronously. We find our VND model to be more flexible for modeling different kinds of dependency structures.

## 2 Theoretical framework

We begin with a discussion of conditions for the sum process  $(S_k)_{k \in \mathbb{N}}$  to be again a homogeneous Markov chain. For this the lumping property turns out to be a sufficient criterion, see (Kemeny and Snell, 1976, Chapter 6.3).

### 2.1 Lumping property

We start with providing terminology, notation and some further tools. For  $x \in \{0, 1\}^\ell$ , let  $x = (x^{(1)}, \dots, x^{(\ell)})^T$  and define the 1-norm by  $\|x\|_1 := \sum_{i=1}^\ell |x^{(i)}|$ , which denotes the number of non-zero entries of  $x$ . Further, for  $m \in [\ell]$  let

$$\mathcal{Z}_m := \{z \in \{0, 1\}^\ell : \|z\|_1 = m\}. \quad (5)$$

**Definition 2.1** (Lumping property). We say that  $(X_k)_{k \in \mathbb{N}_0}$  satisfies the lumping property if for any  $k \in \mathbb{N}$ ,  $i, j \in [\ell]$  and  $x, y \in \mathcal{Z}_i$  holds

$$\mathbb{P}(S_{k+1} = j \mid X_k = x) = \mathbb{P}(S_{k+1} = j \mid X_k = y),$$

whenever  $\mathbb{P}(X_k = y) \cdot \mathbb{P}(X_k = x) > 0$ .

We provide an equivalent characterization for completeness proven in Supplement B.1.

**Lemma 2.2.** *For  $(X_k)_{k \in \mathbb{N}_0}$  satisfying the lumping property is equivalent to*

$$\mathbb{P}(S_{k+1} = j \mid S_k = m) = \mathbb{P}(S_{k+1} = j \mid X_k = x) \quad (6)$$

*for any  $k \in \mathbb{N}$ ,  $j, m \in [\ell]$  and any  $x \in \mathcal{Z}_m$  whenever  $\mathbb{P}(S_k = m) \cdot \mathbb{P}(X_k = x) > 0$ .*

For convenience of the reader we prove in Supplement B.2 that the lumping property reveals  $(S_k)_{k \in \mathbb{N}}$  as a Markov chain again, see also (Kemeny and Snell, 1976, Theorem 6.3.2).

**Proposition 2.3.** *The sequence of random variables  $(S_k)_{k \in \mathbb{N}}$  is a homogeneous Markov chain if  $(X_k)_{k \in \mathbb{N}_0}$  satisfies the lumping property.*

An immediate consequence of the previous lemma and proposition is the following important result.

**Theorem 2.4.** *Let  $M = (m_{x,y})_{x,y \in \{0,1\}^\ell}$  be the transition matrix of the Markov chain  $(X_k)_{k \in \mathbb{N}_0}$ . If  $(X_k)_{k \in \mathbb{N}_0}$  satisfies the lumping property, then  $(S_k)_{k \in \mathbb{N}}$  is a Markov chain with transition matrix  $Q = (q_{i,j})_{i,j \in [\ell]}$  given by*

$$q_{i,j} = \sum_{y \in \mathcal{Z}_j} m_{x,y} \quad (7)$$

*for arbitrary  $x \in \mathcal{Z}_i$ .*

**Remark 2.5.** The fact that  $(X_k)_{k \in \mathbb{N}_0}$  satisfies the lumping property implies that the corresponding transition matrix  $M$  is determined by  $2^\ell(2^\ell - 1) - \ell(2^\ell - 1 - \ell)$  free entries. This means that the lumping property reduces the number of free parameters by  $\ell(2^\ell - 1 - \ell)$  compared to the  $2^\ell(2^\ell - 1)$  free entries of the transition matrix for the general case. However, the number of parameters remains of the order  $\mathcal{O}(2^\ell)$ .

For illustration purposes we show the reduction of the parameters in the case  $\ell = 2$ .

**Example 2.6.** Let  $\ell = 2$  and  $M$  be the transition matrix of  $(X_k)_{k \in \mathbb{N}_0}$ . Then  $M$  can be parametrized by

$$M = \begin{pmatrix} m_{(0,0),(0,0)} & m_{(0,0),(1,0)} & m_{(0,0),(0,1)} & m_{(0,0),(1,1)} \\ m_{(1,0),(0,0)} & m_{(1,0),(1,0)} & m_{(1,0),(0,1)} & m_{(1,0),(1,1)} \\ m_{(0,1),(0,0)} & m_{(0,1),(1,0)} & m_{(0,1),(0,1)} & m_{(0,1),(1,1)} \\ m_{(1,1),(0,0)} & m_{(1,1),(1,0)} & m_{(1,1),(0,1)} & m_{(1,1),(1,1)} \end{pmatrix}, \quad (8)$$

with  $m_{x,(1,1)} = 1 - \sum_{y \neq (1,1)} m_{x,y}$  for all  $x \in \{0,1\}^\ell$ . According to Theorem 2.4, if we assume the lumping property is satisfied, then we have the following extra conditions

$$\begin{aligned} m_{(1,0),(0,0)} &= m_{(0,1),(0,0)} \\ m_{(1,0),(1,0)} + m_{(1,0),(0,1)} &= m_{(0,1),(1,0)} + m_{(0,1),(0,1)} \end{aligned}$$

which reduces the number of free entries from 12 to 10.

## 2.2 Permutation invariance

In this section we elaborate on permutation invariance of a vector Markov chain  $(X_k)_{k \in \mathbb{N}_0}$ , as defined in Definition 1.2. In particular, we show that it implies the lumping property. We also discuss the number of free entries or parameters which determine the transition matrix of a Markov chain with this property. Recall that permutation invariance means that relabeling of the coordinates of the vector Markov chain  $(X_k)_{k \in \mathbb{N}_0}$  does not change the distribution. The following proposition is proven in Supplement B.3.

**Proposition 2.7.** *If  $(X_k)_{k \in \mathbb{N}_0}$  is permutation invariant, it satisfies the lumping property.*

The converse of Proposition 2.7 is in general not true, thus permutation invariance can be considered as stronger than the lumping property. However, it is more accessible in the sense that it is easier to verify and has a more direct interpretation. Permutation invariance can lead to a considerable simplification of the transition matrix of the Markov chain  $(X_k)_{k \in \mathbb{N}_0}$ , which we justify in the following. For this we provide an auxiliary result proven in Supplement B.4.

**Lemma 2.8.** *For  $x_1, y_1, x_2, y_2 \in \{0,1\}^\ell$  with*

$$\|x_1\|_1 = \|x_2\|_1, \quad \|y_1\|_1 = \|y_2\|_1, \quad \text{and} \quad \|x_1 - y_1\|_1 = \|x_2 - y_2\|_1, \quad (9)$$

*there exists a permutation matrix  $P \in \{0,1\}^{\ell \times \ell}$  such that*

$$x_1 = Px_2 \quad \text{and} \quad y_1 = Py_2. \quad (10)$$

*In particular, this implies for a permutation invariant Markov chain  $(X_k)_{k \in \mathbb{N}_0}$  that*

$$\mathbb{P}(X_{k+1} = y_1 \mid X_k = x_1) = \mathbb{P}(X_{k+1} = y_2 \mid X_k = x_2), \quad k \in \mathbb{N}_0.$$

The previous lemma indicates that the number of parameters of the transition matrix of a permutation invariant Markov chain can be bounded by  $(\ell + 1)^3$ . Specifically, in Supplement B.5 we show the following.

**Proposition 2.9.** *The transition matrix  $M$  of a permutation invariant Markov chain is determined by  $\ell(\ell + 1)(\ell + 5)/6$  parameters.*

This means that the property of permutation invariance reduces the number of parameters which determine the entries of  $M$  for a vector Markov chain from an exponential number in  $\ell$  to the order  $\mathcal{O}(\ell^3)$ . Thus, it has significantly less free entries/independent parameters which eases estimation of each parameter significantly. For illustrative purposes we consider  $\ell = 2$  in the following example.

**Example 2.10.** Let  $\ell = 2$  and  $M$  be the transition matrix of  $(X_k)_{k \in \mathbb{N}_0}$ . Then  $M$  can be parametrized as in (8). If we have permutation invariance we obtain the extra conditions

$$\begin{aligned} m_{(0,0),(1,0)} &= m_{(0,0),(0,1)} \\ m_{(1,0),(0,0)} &= m_{(0,1),(0,0)} \\ m_{(1,0),(1,0)} &= m_{(0,1),(0,1)} \\ m_{(1,0),(0,1)} &= m_{(0,1),(1,0)} \\ m_{(1,1),(1,0)} &= m_{(1,1),(0,1)}, \end{aligned}$$

which reduce the number of free entries from 12 to 7.

**Remark 2.11.** For all  $\ell \geq 2$  we have  $\ell(\ell + 1)(\ell + 5)/6 > \ell(\ell + 1)$ . Therefore, the transition matrix of a permutation invariant Markov chain  $(X_k)_{k \in \mathbb{N}_0}$  roughly has about  $\ell/6$  more free entries/parameters than the corresponding transition matrix of the resulting “sum” Markov chain  $(S_k)_{k \in \mathbb{N}}$ . Having our ion channel interpretation in mind this shows that permutation invariance is not sufficient for the transition probabilities of the individual channel currents to be fully determined by the transition probabilities of the sum current.

Now we provide three examples of Markov chains  $(X_k)_{k \in \mathbb{N}_0}$  which are permutation invariant and therefore also satisfy the lumping property. Those scenarios also appear in Chung and Kennedy (1996).

**Example 2.12** (Fully coupled case). Suppose for any  $i \in [\ell]$  that

$$(X_k^{(i)})_{k \in \mathbb{N}_0} = (X_k^{(1)})_{k \in \mathbb{N}_0}.$$

This corresponds to having a vector Markov chain  $(X_k)_{k \in \mathbb{N}_0}$  which is completely determined by  $(X_k^{(1)})_{k \in \mathbb{N}_0}$  where the entries of  $X_k$  are just copies of  $X_k^{(1)}$ . Note here that  $X_k \in \{(0, \dots, 0)^T, (1, \dots, 1)^T\}$  for any  $k \in \mathbb{N}$ . We refer to this scenario as the fully coupled case. Thus, the transition matrix, denoted by  $M^{(\text{FC})} = (m_{x,y}^{(\text{FC})})_{x,y \in \{0,1\}^\ell}$ , of  $(X_k)_{k \in \mathbb{N}_0}$  is given by

$$m_{x,y}^{(\text{FC})} = \begin{cases} 0 & \text{for } y \notin \{(0, \dots, 0)^T, (1, \dots, 1)^T\} \\ \mathbb{P}(X_{k+1}^{(1)} = 0 \mid X_k^{(1)} = 0) & \text{for } x^{(1)} = y^{(1)} = 0 \\ \mathbb{P}(X_{k+1}^{(1)} = 1 \mid X_k^{(1)} = 0) & \text{for } x^{(1)} = 0, y^{(1)} = 1 \\ \mathbb{P}(X_{k+1}^{(1)} = 0 \mid X_k^{(1)} = 1) & \text{for } x^{(1)} = 1, y^{(1)} = 0 \\ \mathbb{P}(X_{k+1}^{(1)} = 1 \mid X_k^{(1)} = 1) & \text{for } x^{(1)} = y^{(1)} = 1, \end{cases}$$

where  $x = (x^{(1)}, \dots, x^{(\ell)})^T$  and  $y = (y^{(1)}, \dots, y^{(\ell)})^T$  with  $x, y \in \{0, 1\}^\ell$ . Either  $X_k \in \mathcal{Z}_0$  or  $X_k \in \mathcal{Z}_\ell$  for any  $k \in \mathbb{N}$ , and therefore,  $S_k \in \{0, \ell\}$ . In this case permutation invariance follows trivially.

**Example 2.13** (Uncoupled case). Let the Markov chains  $(X_k^{(1)})_{k \in \mathbb{N}_0}, \dots, (X_k^{(\ell)})_{k \in \mathbb{N}_0}$  be independent identically distributed, such that each transition matrix is specified by  $\lambda, \eta \in (0, 1)$  with

$$\mathbb{P}(X_{k+1}^{(i)} = 0 \mid X_k^{(i)} = 0) := \lambda, \quad \mathbb{P}(X_{k+1}^{(i)} = 1 \mid X_k^{(i)} = 1) := \eta$$

for all  $i \in [\ell]$ . Thus, the entries of the vector process  $(X_k)_{k \in \mathbb{N}_0}$  are independent. We refer to this scenario as the uncoupled case. For the transition matrix, denoted by  $M^{(\text{UC})} = (m_{x,y}^{(\text{UC})})_{x,y \in \{0,1\}^\ell}$ , of the Markov chain  $(X_k)_{k \in \mathbb{N}_0}$  we have

$$m_{x,y}^{(\text{UC})} = \lambda^{|\{i: x^{(i)}=y^{(i)}=0\}|} (1-\lambda)^{|\{i: x^{(i)}=0, y^{(i)}=1\}|} \eta^{|\{i: x^{(i)}=y^{(i)}=1\}|} (1-\eta)^{|\{i: x^{(i)}=1, y^{(i)}=0\}|},$$

where  $x = (x^{(1)}, \dots, x^{(\ell)})^T$ ,  $y = (y^{(1)}, \dots, y^{(\ell)})^T$  with  $x, y \in \{0, 1\}^\ell$ , and the cardinality of a set  $A$  is denoted by  $|A|$ . For any permutation matrix  $P \in \{0, 1\}^{\ell \times \ell}$  note that

$$m_{x,y}^{(\text{UC})} = m_{Px,Py}^{(\text{UC})}, \tag{11}$$

such that the permutation invariance property holds.

**Example 2.14** (Linear coupling). A combination of the previous two examples is also possible. For  $\kappa \in [0, 1]$ , suppose that the transition matrix of  $(X_k)_{k \in \mathbb{N}_0}$ ,  $M^{(\text{CK})} = (m_{x,y}^{(\text{CK})})_{x,y \in \{0,1\}^\ell}$  (Chung and Kennedy, 1996), is given by

$$M^{(\text{CK})} = \kappa M^{(\text{FC})} + (1 - \kappa) M^{(\text{UC})}.$$

By the fact that the permutation invariance property holds in the previous examples we have for any  $x, y \in \mathcal{Z}_i$  and permutation matrix  $P \in \{0, 1\}^{\ell \times \ell}$  that

$$\begin{aligned} \mathbb{P}(X_{k+1} = y \mid X_k = x) &= \kappa m_{x,y}^{(\text{FC})} + (1 - \kappa) m_{x,y}^{(\text{UC})} = \kappa m_{Px,Py}^{(\text{FC})} + (1 - \kappa) m_{Px,Py}^{(\text{UC})} \\ &= \mathbb{P}(X_{k+1} = Py \mid X_k = Px). \end{aligned}$$

Thus, the Markov chain  $(X_k)_{k \in \mathbb{N}_0}$  with transition matrix  $M$  is permutation invariant.

We discuss now more sophisticated settings of an aggregated state dependency of a Markov chain  $(X_k)_{k \in \mathbb{N}_0}$  which satisfies the lumping property.

## 2.3 Vector norm dependency

A vector norm dependency structure as introduced in Definition 1.1 refers to the fact that the entries of  $X_{k+1}$  of the vector Markov chain  $(X_k)_{k \in \mathbb{N}_0}$  might depend on  $\|X_k\|_1$ , that is, a transition from the  $i$ th entry  $X_k^{(i)}$  to  $X_{k+1}^{(i)}$  is allowed to depend in an explicit way on  $\|X_k\|_1$ .

**Remark 2.15.** For a vector norm dependent Markov chain with transition matrix  $M^{(\text{VND})} = (m_{x,y}^{(\text{VND})})_{x,y \in \{0,1\}^\ell}$ , equation (1) says that for all  $i, j \in \{1, \dots, \ell\}$ ,  $r \in [\ell]$ ,  $k \in \mathbb{N}_0$  and  $b \in \{0, 1\}$  the following holds

$$\mathbb{P}\left(X_{k+1}^{(i)} = b \mid X_k^{(i)} = b, \|X_k\|_1 = r\right) = \mathbb{P}\left(X_{k+1}^{(j)} = b \mid X_k^{(j)} = b, \|X_k\|_1 = r\right).$$

Let  $\lambda_0, \dots, \lambda_{\ell-1}, \eta_1, \dots, \eta_\ell \in [0, 1]$  be parameters according to equations (3) and (4). Now, for  $r \in \{0, \dots, \ell - 1\}$  it follows from equation (2) that

$$\begin{aligned} m_{x,y}^{(\text{VND})} &= \lambda_r^{|\{i: x^{(i)}=y^{(i)}=0\}|} (1 - \lambda_r)^{|\{i: x^{(i)}=0, y^{(i)}=1\}|} \\ &\quad \times \eta_{r+1}^{|\{i: x^{(i)}=y^{(i)}=1\}|} (1 - \eta_{r+1})^{|\{i: x^{(i)}=1, y^{(i)}=0\}|}, \end{aligned} \quad (12)$$

where  $x = (x^{(1)}, \dots, x^{(\ell)})^T$  and  $y = (y^{(1)}, \dots, y^{(\ell)})^T$  with  $x, y \in \{0, 1\}^\ell$ . Thus, the entries of  $M^{(\text{VND})}$  are determined by the  $2\ell$  numbers  $\lambda_0, \dots, \lambda_{\ell-1}, \eta_1, \dots, \eta_\ell$  and, in this sense, the number of parameters is  $2\ell$ . This is, for instance, in contrast to Example 2.13 where only two parameters determine the transition matrix  $M^{(\text{UC})}$ .

From the observation derived in equation (12) we immediately get the following result.

**Proposition 2.16.** *A vector norm dependent Markov chain  $(X_k)_{k \in \mathbb{N}_0}$  is permutation invariant.*

Now, we approach the characterization of norm dependent Markov chains as put forth in Theorem 1.4. Recall the conditional independence property introduced in Definition 1.3, which means that the dependencies within a transition from  $X_k$  to  $X_{k+1}$  of the Markov chain are mediated only by  $X_k$  and not by instantaneous interactions within the entries of  $X_{k+1}$ .

The following technical lemma will be used in the proof of Theorem 1.4. It is proven in Supplement B.6.

**Lemma 2.17.** *Let  $(X_k)_{k \in \mathbb{N}_0}$  be a permutation invariant vector Markov chain with permutation invariant initial distribution, that is,*

$$\mathbb{P}(X_0 = y) = \mathbb{P}(X_0 = Py), \quad (13)$$

*for any permutation matrix  $P \in \{0, 1\}^{\ell \times \ell}$  and any  $y \in \{0, 1\}^\ell$ . Then, for any  $i \in \{1, \dots, \ell\}$ ,  $x \in \{0, 1\}^\ell$  and  $k \in \mathbb{N}_0$  we have*

$$\mathbb{P}(X_{k+1}^{(i)} = y^{(i)} \mid X_k = x) = \mathbb{P}(X_{k+1}^{(i)} = y^{(i)} \mid X_k^{(i)} = x^{(i)}, \|X_k\|_1 = \|x\|_1) \quad (14)$$

*with  $x = (x^{(1)}, \dots, x^{(\ell)})^T$  and  $y = (y^{(1)}, \dots, y^{(\ell)})^T$ .*

An immediate consequence is the following.

**Remark 2.18.** Under the assumptions of the previous lemma we have by the fact that  $(X_k)_{k \in \mathbb{N}_0}$  is a homogeneous Markov chain that the expression

$$\mathbb{P}(X_{k+1}^{(i)} = y^{(i)} \mid X_k^{(i)} = x^{(i)}, \|X_k\|_1 = \|x\|_1)$$

is independent of  $k \in \mathbb{N}_0$ .

Now we have all the tools for proving the VND characterization, of Theorem 1.4.

*Proof of Theorem 1.4.* By Proposition 2.16 a vector norm dependent Markov chain is permutation invariant. Furthermore, by the definition of vector norm dependence and Lemma 2.17 the conditional independence property is satisfied.

We turn to the other direction. Let  $(X_k)_{k \in \mathbb{N}_0}$  be permutation invariant and conditionally independent. Then, for all  $x, y \in \{0, 1\}^\ell$  we have

$$\mathbb{P}(X_{k+1} = y \mid X_k = x) = \prod_{i=1}^{\ell} \mathbb{P}(X_{k+1}^{(i)} = y^{(i)} \mid X_k = x),$$

such that by Lemma 2.17 the equality of (2) follows. By Remark 2.18, the transition probabilities (1) of Definition 1.1 are constant in  $k$ , so that we only need to argue that they are also constant w.r.t.  $i \in \{1, \dots, \ell\}$ . Let  $y_i, \bar{y}_i \in \{0, 1\}^\ell$  with

$$\begin{aligned} y_i &= (y^{(1)}, \dots, y^{(i-1)}, 1, y^{(i+1)}, \dots, y^{(\ell)})^T, \\ \bar{y}_i &= (y^{(1)}, \dots, y^{(i-1)}, 0, y^{(i+1)}, \dots, y^{(\ell)})^T, \end{aligned}$$

that is,  $y_i$  and  $\bar{y}_i$  differ only in the  $i$ th entry of the vector. Furthermore, let  $P_{i,j} \in \{0, 1\}^\ell$  be the permutation which only permutes the  $i$ -th and  $j$ -th entry of a vector. Then for any  $x \in \{0, 1\}^\ell$  with  $x = (x^{(1)}, \dots, x^{(\ell)})^T$  we have

$$\begin{aligned} & \frac{\mathbb{P}(X_{k+1}^{(i)} = 1 \mid X_k^{(i)} = x^{(i)}, \|X_k\|_1 = \|x\|_1)}{\mathbb{P}(X_{k+1}^{(i)} = 0 \mid X_k^{(i)} = x^{(i)}, \|X_k\|_1 = \|x\|_1)} \stackrel{(14)}{=} \frac{\mathbb{P}(X_{k+1}^{(i)} = y_i^{(i)} \mid X_k = x)}{\mathbb{P}(X_{k+1}^{(i)} = \bar{y}_i^{(i)} \mid X_k = x)} \\ &= \frac{\prod_{j=1}^{\ell} \mathbb{P}(X_{k+1}^{(j)} = y_i^{(j)} \mid X_k = x)}{\prod_{j=1}^{\ell} \mathbb{P}(X_{k+1}^{(j)} = \bar{y}_i^{(j)} \mid X_k = x)} = \frac{\mathbb{P}(X_{k+1} = y_i \mid X_k = x)}{\mathbb{P}(X_{k+1} = \bar{y}_i \mid X_k = x)} \\ &= \frac{\mathbb{P}(X_{k+1} = P_{i,j} y_i \mid X_k = P_{i,j} x)}{\mathbb{P}(X_{k+1} = P_{i,j} \bar{y}_i \mid X_k = P_{i,j} x)} = \frac{\prod_{j=1}^{\ell} \mathbb{P}(X_{k+1}^{(j)} = P_{i,j} y_i^{(j)} \mid X_k = P_{i,j} x)}{\prod_{j=1}^{\ell} \mathbb{P}(X_{k+1}^{(j)} = P_{i,j} \bar{y}_i^{(j)} \mid X_k = P_{i,j} x)} \\ &= \frac{\mathbb{P}(X_{k+1}^{(j)} = (P_{i,j} y_i)^{(j)} \mid X_k = P_{i,j} x)}{\mathbb{P}(X_{k+1}^{(j)} = (P_{i,j} \bar{y}_i)^{(j)} \mid X_k = P_{i,j} x)} \stackrel{(14)}{=} \frac{\mathbb{P}(X_{k+1}^{(j)} = 1 \mid X_k^{(j)} = x^{(i)}, \|X_k\|_1 = \|x\|_1)}{\mathbb{P}(X_{k+1}^{(j)} = 1 \mid X_k^{(j)} = x^{(i)}, \|X_k\|_1 = \|x\|_1)}, \end{aligned}$$

where we used the conditional independence and permutation invariance. Taking into account that for any  $j \in \{1, \dots, \ell\}$  holds

$$\begin{aligned} & \mathbb{P}(X_{k+1}^{(j)} = 1 \mid X_k^{(j)} = x^{(i)}, \|X_k\|_1 = \|x\|_1) \\ &+ \mathbb{P}(X_{k+1}^{(j)} = 0 \mid X_k^{(j)} = x^{(i)}, \|X_k\|_1 = \|x\|_1) = 1, \end{aligned}$$

leads in particular for any  $i, j \in \{1, \dots, \ell\}$ ,  $r \in [\ell]$  and  $b \in \{0, 1\}$  to

$$\mathbb{P}(X_{k+1}^{(i)} = b \mid X_k^{(i)} = b, \|X_k\|_1 = r) = \mathbb{P}(X_{k+1}^{(j)} = b \mid X_k^{(j)} = b, \|X_k\|_1 = r),$$

which finishes the proof.  $\square$



We end this section by providing a representation of the transition matrix of the “sum” Markov chain  $(S_k)_{k \in \mathbb{N}}$  based on a vector norm dependent Markov chain  $(X_k)_{k \in \mathbb{N}_0}$ . For the proof of the following result we refer to Supplement B.7.

**Proposition 2.19.** *Given a vector norm dependent Markov chain  $(X_k)_{k \in \mathbb{N}_0}$  with transition matrix  $M^{(\text{VND})}$  determined by the parameters  $\lambda_0, \dots, \lambda_{\ell-1}, \eta_1, \dots, \eta_\ell \in [0, 1]$ , see Remark 2.15. Then, the transition matrix  $Q = (q_{i,j})_{i,j \in [\ell]}$  of the corresponding “sum” Markov chain  $(S_k)_{k \in \mathbb{N}}$  is given by*

$$q_{i,j} := \sum_{r=\max\{0, i-j\}}^{\min\{i, \ell-j\}} \binom{i}{r} \binom{\ell-i}{j-i+r} \eta_i^{i-r} (1-\eta_i)^r \lambda_i^{\ell-j-r} (1-\lambda_i)^{j-i+r},$$

for any  $i, j \in [\ell]$ , where for completeness we set  $\eta_0 := 1$  and  $\lambda_\ell := 1$ .

## 2.4 Inverse lumping and identifiability

Let  $(X_k)_{k \in \mathbb{N}_0}$  be a vector Markov chain on  $\{0, 1\}^\ell$  with transition matrix  $M = (m_{x,y})_{x,y \in \{0,1\}^\ell}$ . Suppose that  $(X_k)_{k \in \mathbb{N}_0}$  satisfies the lumping property and therefore the corresponding “sum” process  $(S_k)_{k \in \mathbb{N}}$  is a Markov chain with transition matrix  $Q = (q_{i,j})_{i,j \in [\ell]}$ , see Theorem 2.4. The transition matrix  $Q$  is completely determined by  $M$ , see equation (7). This fact has been already used in Chung and Kennedy (1996) leading to the Chung-Kennedy model in Example 2.14. However, we are interested in reversing the perspective. Namely, we ask the following question: *Can we uniquely recover  $M$  from  $Q$ ?* We refer to this as the *inverse lumping problem*.

Without further conditions on  $(X_k)_{k \in \mathbb{N}_0}$  this is not possible. Indeed the lumping property is not sufficient and even if we have permutation invariance we know from Proposition 2.9 that the number of parameters determining  $M$  is  $\ell(\ell+1)(\ell+5)/6$ , which is larger than the number of parameters that determine  $Q$ . This shows that the property of permutation invariance is not sufficient for an affirmative answer to the inverse lumping problem. We illustrate this in the case  $\ell = 2$ .

**Example 2.20.** Consider the same setting as in Example 2.10, i.e., let  $(X_k)_{k \in \mathbb{N}_0}$  be a permutation invariant Markov chain and  $Q$  be the transition matrix of  $(S_k)_{k \in \mathbb{N}}$ . Then, by Theorem 2.4 we have

$$Q = \begin{pmatrix} m_{(0,0),(0,0)} & 2m_{(0,0),(1,0)} & m_{(0,0),(1,1)} \\ m_{(1,0),(0,0)} & m_{(1,0),(1,0)} + m_{(1,0),(0,1)} & m_{(1,0),(1,1)} \\ m_{(1,1),(0,0)} & 2m_{(1,1),(1,0)} & m_{(1,1),(1,1)} \end{pmatrix}.$$

Note that  $Q$  is parametrized with 7 parameters. In particular, knowing  $Q$  the transition matrix  $M$  cannot be fully recovered, since we are not able to identify  $m_{(1,0),(1,0)}$  and  $m_{(1,0),(0,1)}$ .

This shows the need to add structural assumptions on  $(X_k)_{k \in \mathbb{N}_0}$ . Suppose now that  $(X_k)_{k \in \mathbb{N}_0}$  is permutation invariant and conditional independent. Then, for

suitable initial distributions, this leads to a vector norm dependent Markov chain, see Theorem 1.4. The number of parameters determining  $M$  in this setting is  $2\ell$ , see Remark 2.15, which is smaller or equal than  $\ell(\ell + 1)$ . Therefore, a solution of the inverse lumping problem is not immediately excluded. Indeed, we find that the parameters can be uniquely determined as stated in Theorem 1.5, which is proven in Supplement B.8.

Using equation (2), this means for a VND Markov chain we can recover the transition matrix  $M^{(\text{VND})}$  from the transition matrix  $Q^{(\text{VND})}$  of the corresponding “sum” process. This paves the way for estimating these parameters from data, which we adress in the following section. In the setting of the previous theorem we can therefore give an affirmative answer to the question of the inverse lumping problem.

### 3 VND Hidden Markov model estimation

We provide a short review on homogeneous HMM, define basic concepts and explain our HMM setting. Additionally, we introduce a customized Baum-Welch algorithm, which is adjusted to account for our specific modeling.

#### 3.1 VND Hidden Markov model and vector norm dependency

Assume that the measurable space  $(\Omega, \mathcal{F})$  is equipped with a family of probability measures  $(\mathbb{P}_\theta)_{\theta \in \Theta}$ , where  $\Theta \subseteq \mathbb{R}^d$  for some  $d \in \mathbb{N}$  denotes an underlying parameter set. Let  $\ell \in \mathbb{N}$  (e.g., corresponding to the number of channels) and let  $(S_k, Y_k)_{k \in \mathbb{N}}$  be a bivariate stochastic process defined on  $(\Omega, \mathcal{F})$ , where  $(S_k)_{k \in \mathbb{N}}$  is a Markov chain on the finite state space  $[\ell]$  and  $(Y_k)_{k \in \mathbb{N}}$ , conditioned on  $(S_k)_{k \in \mathbb{N}}$ , is a real-valued, independent sequence of random variables. Taking the parametrized family of probability distributions into account, this leads to a parametrized (homogeneous) HMM  $(S_k, Y_k)_{k \in \mathbb{N}}$ . Given observed data  $y_1, \dots, y_K \in \mathbb{R}$  for  $K \in \mathbb{N}$ , i.e., realizations of  $Y_1, \dots, Y_K$ , the goal is to determine the “true” underlying parameter  $\theta^* \in \Theta$ . In this context we call  $(S_k)_{k \in \mathbb{N}}$  the hidden Markov chain and the distribution of  $Y_k$  given  $S_k$  the *emission distribution*. Furthermore, assume that the parameter set can be represented as  $\Theta = \Theta_H \times \Theta_E$ , where  $\Theta_H$  corresponds to the part of the parameters which come from the hidden Markov chain and  $\Theta_E$  denotes the part which comes from the emission distribution.

Suppose now that  $(S_k)_{k \in \mathbb{N}}$  is the “sum” process based on a vector norm dependent Markov chain  $(X_k)_{k \in \mathbb{N}}$  on  $\{0, 1\}^\ell$ . Set  $\Theta_H = [0, 1]^{2\ell}$ , such that an element  $\theta_H \in \Theta_H$  is given by  $\theta_H = (\lambda_0, \dots, \lambda_{\ell-1}, \eta_1, \dots, \eta_\ell)$ , where  $\lambda_r$  and  $\eta_{r+1}$  with  $r = 0, \dots, \ell - 1$  determine the transition matrix  $Q^{(\text{VND})}(\theta_H) = (q_{i,j}^{(\text{VND})}(\theta_H))_{i,j \in [\ell]}$  of the Markov chain  $(S_k)_{k \in \mathbb{N}}$  as in Proposition 2.19. In formulas, for any  $k \in \mathbb{N}$  and any  $\theta \in \Theta$  we have

$$\mathbb{P}_\theta(S_{k+1} = s_{k+1} \mid S_k = s_k, \dots, S_1 = s_1) = \mathbb{P}_\theta(S_{k+1} = s_{k+1} \mid S_k = s_k) = q_{s_k, s_{k+1}}^{(\text{VND})}(\theta_H),$$

where  $(s_1, \dots, s_{k+1}) \in [\ell]^{k+1}$  and  $\theta = (\theta_H, \theta_E) \in \Theta$ . In particular, note that the transition matrix  $Q^{(\text{VND})}(\theta_H)$  does not depend on  $k$ , which means that the hidden Markov chain is homogeneous.

Additionally, for  $\theta_E \in \Theta_E$  we assume that the emission distribution is determined by a strictly positive probability Lebesgue density function  $g_{\theta_E}: \mathbb{R} \times [\ell] \rightarrow (0, \infty)$ , such that

$$\begin{aligned} \mathbb{P}_\theta(Y_k \in A \mid S_k = s_k, \dots, S_1 = s_1, Y_{k-1} = y_{k-1}, \dots, Y_1 = y_1) &= \mathbb{P}_\theta(Y_k \in A \mid S_k = s_k) \\ &= \int_A g_{\theta_E}(y, s_k) \, dy, \end{aligned}$$

for any  $k \in \mathbb{N} \setminus \{1\}$ ,  $(s_1, \dots, s_k)^T \in [\ell]^k$ ,  $(y_1, \dots, y_{k-1})^T \in \mathbb{R}^{k-1}$ , any Borel set  $A \subseteq \mathbb{R}$  and  $\theta = (\theta_H, \theta_E) \in \Theta$ . Let us emphasize here that we consider only homogeneous emission measures, i.e.,  $g_{\theta_E}$  does not depend on  $k$  (in contrast to the considerations in Diehn et al. (2019)). As a concrete setting, we provide a Gaussian standard scenario.

**Example 3.1.** With  $\mathcal{N}(m, v^2)$  and  $m \in \mathbb{R}$  as well as  $v > 0$  we denote the normal distribution with mean  $m$  and variance  $v^2$ . Let  $\Theta_E = \mathbb{R}^2 \times (0, \infty)^{\ell+1}$  and  $\theta_E \in \Theta_E$  with  $\theta_E = (\mu, \nu, \sigma_0, \dots, \sigma_\ell)$ . For  $k \in \mathbb{N}$  consider

$$Y_k = \mu + S_k \nu + \sigma_{S_k} \xi$$

with  $\xi \sim \mathcal{N}(0, 1)$ , i.e.,  $Y_k \sim \mathcal{N}(\mu + S_k \nu, \sigma_{S_k}^2)$ . Therefore, for any  $j \in [\ell]$  we have

$$g_{\theta_E}(y, j) = \frac{1}{\sqrt{2\pi\sigma_j^2}} \exp\left(-\frac{|y - \mu - j\nu|^2}{2\sigma_j^2}\right).$$

Assume that  $\pi = (\pi^{(0)}, \dots, \pi^{(\ell)}) \in [0, 1]^{[\ell]}$  is the probability vector that provides the initial distribution of the Markov chain  $(S_k)_{k \in \mathbb{N}}$ . By convention, let  $\mathbb{P}_\theta(S_1 = s \mid S_0) := \pi^{(s)}$  for any  $s \in [\ell]$ . For simplicity, we assume  $\pi$  to be known. Furthermore, to shorten the notation for a finite sequence  $z_1, \dots, z_K$  we write  $z_{1:K}$ . (Thus, the event  $\{S_{1:K} = s_{1:K}\}$  coincides with  $\{S_1 = s_1, \dots, S_K = s_K\}$ .) Then, the probability of  $Y_{1:K}$  from the HMM being in a Borel set  $A \subseteq \mathbb{R}^K$  is determined by

$$\begin{aligned} \mathbb{P}_\theta(S_{1:K} = s_{1:K}, Y_{1:K} \in A) &= \int_A \prod_{k=1}^K g_{\theta_E}(y_k, s_k) \mathbb{P}_\theta(S_k = s_k \mid S_{k-1} = s_{k-1}) \, dy_{1:K} \\ &= \int_A g_{\theta_E}(y_1, s_1) \pi^{(s_1)} \times \prod_{k=2}^K g_{\theta_E}(y_k, s_k) q_{s_{k-1}, s_k}^{(\text{VND})} \, dy_{1:K}. \quad (15) \end{aligned}$$

### 3.2 Parameter estimation and Baum-Welch algorithm

For parameter estimation within the previously described HMM setting we use the Baum-Welch algorithm, whose convergence was discussed in Baum et al. (1970).

It is based on the expectation maximization (EM) paradigm, which means that an expectation computation step is followed by a maximization step. In order to discuss the algorithm we provide for  $s_{1:K} \in [\ell]^K$  and  $y_{1:K} \in \mathbb{R}^K$  the log-likelihood function  $\theta \mapsto \ell(\theta; s_{1:K}, y_{1:K})$  within our parametrization. From (15) we can deduce for  $\theta = (\theta_H, \theta_E) \in \Theta$  that

$$\ell(\theta, s_{1:K}, y_{1:K}) = \log \pi^{(s_1)} + \sum_{k=1}^{K-1} \log q_{s_k, s_{k+1}}^{(\text{VND})}(\theta_H) + \sum_{k=1}^K \log g_{\theta_E}(y_k, s_k). \quad (16)$$

Note that only in the second term of the log-likelihood function the parametrized components of the transition matrix  $Q^{(\text{VND})}(\theta_H)$  appear. This is in contrast to settings where all  $(\ell + 1)\ell$  entries of possible transition matrices determine the parameters of the hidden Markov chain.

For the convenience of the reader we provide the general form of the Baum-Welch algorithm which leads to a sequence  $(\theta_t)_{t \in \mathbb{N}} \subset \Theta$  that satisfies, under weak assumptions, the convergence to a local maximum of the likelihood function. The following steps with increasing iteration index  $t \in \mathbb{N}$  are performed until a convergence criterion is reached:

1. For all  $k = 1, \dots, K$  compute the so-called univariate and bivariate filtering distributions, given by  $s \mapsto \mathbb{P}_{\theta_t}(S_k = s \mid Y_{1:K} = y_{1:K})$  and  $(r, s) \mapsto \mathbb{P}_{\theta_t}(S_k = r, S_{k+1} = s \mid Y_{1:K} = y_{1:K})$  with  $r, s \in [\ell]$ , by a forward-backward algorithm using the parameter  $\theta_t \in \Theta$  determined in the previous iteration.
2. Expectation step: Given  $\theta_t$  (and of course  $y_{1:K}$ ) define  $\theta \mapsto f(\theta; \theta_t, y_{1:K})$  with  $\theta = (\theta_H, \theta_E) \in \Theta$  by

$$\begin{aligned} f(\theta; \theta_t, y_{1:K}) &= \sum_{k=1}^K \sum_{s_k \in [\ell]} \log g_{\theta_E}(y_k, s_k) \mathbb{P}_{\theta_t}(S_k = s_k \mid Y_{1:K} = y_{1:K}) \\ &+ \sum_{k=1}^{K-1} \sum_{s_k, s_{k+1} \in [\ell]} \log q_{s_k, s_{k+1}}^{(\text{VND})}(\theta_H) \mathbb{P}_{\theta_t}(S_k = s_k, S_{k+1} = s_{k+1} \mid Y_{1:K} = y_{1:K}). \end{aligned}$$

(We obtain this function by taking the expectation of (16) w.r.t. the distribution of  $S_{1:K}$  given  $Y_{1:K} = y_{1:K}$  under  $\mathbb{P}_{\theta_t}$  and neglect multiplicative constants as well as terms that do not depend on  $\theta$ .)

3. Maximization step: Compute  $\theta_{t+1} := \arg \max_{\theta \in \Theta} f(\theta; \theta_t, y_{1:K})$ .

As mentioned above, in Baum et al. (1970), it is shown that this procedure defines a sequence  $(\theta_t)_{t \in \mathbb{N}} \subset \Theta$  that converges under weak assumptions to a local maximum of the likelihood. In particular, in the Gaussian emission distribution setting of Example 3.1 and our VND modeling convergence is achieved. Integrating the parametric form in the expectation step has the benefit that in each iteration the parameters remain in the parameter space. However, there are computational issues in our setting with the third step of the Baum-Welch approach.

Note that we do not obtain a closed expression for  $\theta_{t+1}$ , since the parametric form of  $q_{s_k, s_{k+1}}^{(\text{VND})}(\theta_{t+1})$  is convoluted (see Proposition 2.19). Instead, we propose to solve this maximization problem numerically. In general, the function  $\theta \mapsto f(\theta, \theta_t, y_{1:K})$  does not need to be strictly unimodal, and therefore the maximum may not be unique. From (16) we observe that for strict unimodality it is sufficient to show that  $\sum_{k=1}^{K-1} \log q_{s_k, s_{k+1}}^{(\text{VND})}(\theta_H)$  is strictly unimodal, since the two other terms are strictly concave in the Gaussian case (and any case of emission densities with concave likelihood). Note that this expression is complicated by the fact that the polynomials  $q_{s_k, s_{k+1}}^{(\text{VND})}$  are, in general, sums themselves (see Proposition (2.19)). For  $\ell = 2$  the plots in Figure 6 in Supplement C indicate that  $\sum_{k=1}^{K-1} \log q_{s_k, s_{k+1}}^{(\text{VND})}(\theta_H)$  is in general not strictly unimodal, but a sufficient condition may be to restrict to  $\lambda_1 \geq 1 - \eta_1$  (the same condition as Theorem 1.5).

Moreover, the estimation of the  $\theta_H$ -part of the parameters determines automatically in a unique way the transition matrix  $M^{(\text{VND})}$  of the vector norm dependent Markov chain  $(X_k)_{k \in \mathbb{N}_0}$ , see Theorem 1.5. Using this we can derive estimates (at least for small  $\ell$ ) of  $M^{(\text{VND})}$ .

## 4 Application to ion channels

Ion channels can open and close in order to control the flux of charged ions across the membrane of the cell or intracellular organelles. This process is called *gating*. Gating dynamics of ligand-gated ion channels vary depending on binding-ligand concentration (e.g. the cytosolic and/or intraorganelle luminal  $\text{Ca}^{2+}$  concentration). Here, we model a set of multiple ion channels in an artificial lipid bilayer by a Gaussian emission HMM as explained in Example 3.1. Our goal is to model the multiple channels in the bilayer as well as the dependencies between them. These dependencies are not necessarily caused by direct physical interaction of channels but may be mediated indirectly by joint environment factors, such as an overall increase in  $\text{Ca}^{2+}$  concentration on either side of the membrane.

Our present application is in RyR2 (Ryanodine Receptor type 2) channels found primarily in cardiac muscle cells and neurons. These receptors are important in controlling intracellular  $\text{Ca}^{2+}$  release from the endoplasmatic reticulum during cardiac excitation-contraction coupling. Genetic and proteomic defects in RyR2 lead to abnormally increased resting  $\text{Ca}^{2+}$  release, causing cardiac arrhythmia and contractile dysfunction (Taur and Frishman, 2005; Salvage et al., 2019). Extensive research about the gating mechanism at low levels of  $\text{Ca}^{2+}$  where only single proteins are active at a time has been conducted. The next step is to investigate the dependencies between multiple channels since the probability of subcellular calcium release may depend significantly on those channel dependencies. Several investigations of local channel clustering have been conducted on living cells, cf. (Walker et al., 2014, 2015). While nonindependent gating has been reported for RyR2 channels in some studies, the question if and how positive (cooperative) gating occurs in subcellular channel clusters is not conclusively answered, cf. (Marx

et al., 2001; Laver et al., 2004; Chen et al., 2009; Walker et al., 2014; Williams et al., 2018).

We investigate two data sequences, which were measured subsequently on the same system of wild-type RyR2 channels in a synthetic lipid bilayer with different luminal (trans) concentrations of  $\text{Ca}^{2+}$  ions of 5 mM (data set 1) and 10 mM (data set 2) at a constant cytosolic (cis)  $\text{Ca}^{2+}$  concentration of 150 nM. Additionally, 53 mM  $\text{Ba}^{2+}$  was present on the trans side of the lipid bilayer and used as a principal charge carrier, since higher conductance of RyR2 for  $\text{Ba}^{2+}$  results in better signal-to-noise ratio. Materials and methods are discussed in more detail in Supplement D.1 Finally, to estimate the number of actively gating channels  $\ell$ , the  $\text{Ca}^{2+}$  concentration on the cis side was increased to 5  $\mu\text{M}$  and 1mM of adenosine triphosphate (ATP) was added to fully activate the channels. The maximally elicited transmembrane current was then divided by the single-channel current amplitude. Here, the number of experimentally detected channels results in  $\ell = 20$ . However, we note that during the given measurement time intervals without ATP, the maximum number of channels opening at a time was 2. Therefore, the number of parameters of the emission model reduces to 5.

#### 4.1 Determining a suitable model

We compare and investigate three models. Since visual inspection of the data suggests that no more than two channels are open at any given time, we use  $\ell = 2$  for all three of them. The baseline model, against which we compare the two other models is the model of uncoupled (independent) channels (UC). Here the “sum” Markov chain  $(S_k)_{k \in \mathbb{N}}$  is based on  $(X_k)_{k \in \mathbb{N}_0}$  considered in Example 2.13 and the corresponding transition matrix is given by

$$Q^{(\text{UC})} := \begin{pmatrix} \lambda_0^2 & 2\lambda_0(1 - \lambda_0) & (1 - \lambda_0)^2 \\ \lambda_0(1 - \eta_1) & \lambda_0\eta_1 + (1 - \lambda_0)(1 - \eta_1) & (1 - \lambda_0)\eta_1 \\ (1 - \eta_1)^2 & 2\eta_1(1 - \eta_1) & \eta_1^2 \end{pmatrix}.$$

The other two models are the model from Example 2.14 by Chung and Kennedy (1996) (CK) and our VND model described in Section 3. In the CK model  $(S_k)_{k \in \mathbb{N}}$  is based on the vector Markov chain considered in Example 2.14 and the transition matrix takes the form

$$Q^{(\text{CK})} := (1 - \kappa)Q^{(\text{UC})} + \kappa \begin{pmatrix} \lambda_0 & 0 & (1 - \lambda_0) \\ 1/2 & 0 & 1/2 \\ (1 - \eta_1) & 0 & \eta_1 \end{pmatrix},$$

where additional to the parameters  $\lambda_0$  and  $\eta_1$  a coupling parameter  $\kappa \in [0, 1]$  appears. In the VND model the Markov chain  $(S_k)_{k \in \mathbb{N}}$  is given by the “sum” process based on a vector norm dependent Markov chain, recall Definition 1.1. For  $\ell = 2$  its transition matrix is given

$$Q^{(\text{VND})} := \begin{pmatrix} \lambda_0^2 & 2\lambda_0(1 - \lambda_0) & (1 - \lambda_0)^2 \\ \lambda_1(1 - \eta_1) & \lambda_1\eta_1 + (1 - \lambda_1)(1 - \eta_1) & (1 - \lambda_1)\eta_1 \\ (1 - \eta_2)^2 & 2\eta_2(1 - \eta_2) & \eta_2^2 \end{pmatrix}.$$

Table 1: *Differences of Bayesian information criteria (BIC) between UC and CK model in the first row and UC and VND model in the second row for two ion channel data sequences, provided by the HRCG. The VND clearly yields the smallest BIC, while the added parameter in the CK model does not achieve a sufficient increase in the likelihood to improve the BIC.*

	Data Set 1	Data Set 2
$2(\log L^{(\text{CK})} - \log L^{(\text{UC})}) - 2\ln(K)$	-10.52	-7.49
$2(\log L^{(\text{VND})} - \log L^{(\text{UC})}) - 2\ln(K)$	5979.6	6842.5

Table 2: *Estimated parameters for both data sets. For easier interpretation we display  $1 - \theta$  for every estimated parameter  $\theta$ , since these are probabilities of channels to open or close. From the ratios  $\frac{1-\hat{\lambda}_0}{1-\hat{\lambda}_1}$  and  $\frac{1-\hat{\eta}_2}{1-\hat{\eta}_1}$ , which are all much larger than 1, we can conclude that the gating is strongly competitive.*

	$1 - \hat{\lambda}_0$	$1 - \hat{\lambda}_1$	$\frac{1-\hat{\lambda}_0}{1-\hat{\lambda}_1}$	$1 - \hat{\eta}_1$	$1 - \hat{\eta}_2$	$\frac{1-\hat{\eta}_2}{1-\hat{\eta}_1}$
Data Set 1	0.0123	0.0021	5.834	0.0078	0.0629	8.074
Data Set 2	0.0162	0.0027	6.002	0.0047	0.0457	9.637

The goal of the present section is to determine, whether the CK or the VND model provide a better explanation for the data than the UC model. We use the Bayesian information criterion to compare models.

Table 1 shows that the Chung-Kennedy model, which can only model cooperative gating, does not yield an improvement over uncoupled channels, while the VND model clearly does. In Figure 2 in the introduction we compare a data trace with random sequences generated from the estimated, effectively uncoupled CK model and the VND model.

In summary, one can clearly see that the VND model provides a much better fit than the uncoupled and the CK model, in accordance with the results of the BIC. In order to see whether the estimated parameters  $\hat{\lambda}_0, \hat{\lambda}_2, \hat{\eta}_1, \hat{\eta}_2$  support the conclusion of competitive gating, we investigate the ratios  $\frac{1-\hat{\eta}_2}{1-\hat{\eta}_1}$  and  $\frac{1-\hat{\lambda}_0}{1-\hat{\lambda}_1}$ . For competitive gating, we expect both of these ratios to be  $> 1$  since this would indicate that transitions into the state with one channel open are preferred relative to transitions out of this state. In turn, both ratios being  $< 1$  would indicate cooperative gating.

In Table 2 we see that  $\frac{1-\hat{\lambda}_0}{1-\hat{\lambda}_1} \gg 1$  and  $\frac{1-\hat{\eta}_2}{1-\hat{\eta}_1} \gg 1$  for both data sets, which shows strongly competitive gating. It should be noted that the results discussed here stem from one single experiment. Therefore, a valid biophysical conclusion is above the scope of this article. In particular, the cause of competitive gating in this experimental system is not clear and further research is required to confirm and explain this result. However, since the finding of competitive gating is unexpected,

we contend that it deserves further experimental investigation.

## 4.2 Robustness of results to number of channels

Estimating the number of channels can be difficult using the VND model, as the dependence of the transition matrix on the number of channels is weak. For a discussion and illustration we refer to Supplement D.2. This potentially renders the channel estimation susceptible to distortion by systemic effects like e.g. signal filtering. Therefore, we investigate the converse situation namely how robust results of the VND model are, if the number of channels is underestimated. Note that overestimating the number of channels rarely occurs in practice, if the number of levels of a single channel are (approximately) known.

In order to inspect a situation close to the experimental data, we simulate 1 000 000 data points from a system of 20 channels in the UC model and the VND model with different sets of parameters which were chosen such that the highest number of channels open at the same time was 3. Then we fit a VND model with 3 channels to the data and inspect the estimated parameters for signs of competitive or cooperative gating. In order to acquire variance estimates, 100 repetitions were done for each set of parameters. We investigate the ratios  $\frac{1-\hat{\eta}_2}{1-\hat{\eta}_1}$  and  $\frac{1-\hat{\lambda}_0}{1-\hat{\lambda}_1}$ , where we expect both of these ratios to be  $> 1$  in case of competitive gating since this would indicate that transitions into the state with one channel open are preferred relative to transitions out of this state. In turn, both ratios being  $< 1$  would indicate cooperative gating.

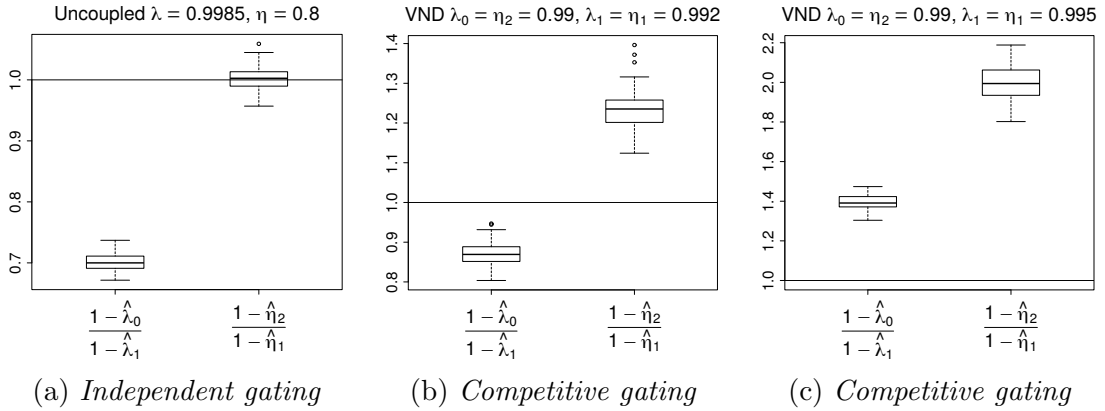


Figure 4: Boxplots displaying ratios of parameters estimated by a 3 channel VND model for 100 repetitions of simulations of  $n = 1\,000\,000$  point from a system with  $\ell = 20$  channels with the given parameters and  $\lambda_k = 1$  for  $k > 1$  and  $\eta_k = 0.8$  for  $k > 2$ . One can see that the estimated ratio  $\frac{1-\hat{\eta}_2}{1-\hat{\eta}_1}$  is very close to the true value in all cases but  $\frac{1-\hat{\lambda}_0}{1-\hat{\lambda}_1}$  is systematically underestimated by a factor of  $\sim 0.7$ .

As is clear from the estimated parameters displayed in Figure 4, the qualitative coupling behavior is recovered. Panel (a) shows that for uncoupled channels the estimated parameters do not clearly point to either competitive or cooperative gating. Panel (c) shows that for competitive gating with  $\frac{1-\lambda_0}{1-\lambda_1} = \frac{1-\eta_2}{1-\eta_1} = 2$ , the



probabilities to transition into state 1 are significantly greater than the probabilities to transition out of this state. This means that the qualitative gating behavior is faithfully recovered even though specific parameter values are not comparable. Panel (b) shows a boundary case of competitive gating with  $\frac{1-\lambda_0}{1-\lambda_1} = \frac{1-\eta_2}{1-\eta_1} = 1.25$ . The result is also compatible with uncoupled gating since  $\frac{1-\hat{\lambda}_0}{1-\hat{\lambda}_1}$  is systematically underestimated by a factor of 0.7.

In conclusion, underestimating the number of channels may lead one to underestimate but not overestimate competitive gating. This underscores the usefulness of the VND model for the identification of coupled gating, even if the number of channels is not exactly known and only a subset of the channels are open at the same time during the observation time span. More specifically, it reinforces the qualitative finding of competitive gating for the ion channels analyzed above as this does not arise as an artifact of underestimating the number of channels.

## 5 Discussion and Outlook

We have introduced a hidden Markov model for the description of a set of possibly coupled emitters, if only the sum of their signals is measured. We distinguish two main types of emitter interaction, namely cooperative and competitive emission. In case of competitive emission, the resulting signal can often exhibit only few states and thereby disguise the true number of emitters. This can lead to an underestimation of the number of emitters, so it is important to note that the VND model we introduce allows to draw the right conclusion whether emitters work cooperatively or competitively even if the number of emitters is underestimated. In summary, the VND model is a powerful tool to distinguish different types of emitter interaction which is robust to underestimation of the number of emitters.

The VND model faces the typical limitations of homogeneous Markov models in that changes in emitter behavior over time cannot be modeled in this setting. Furthermore, the assumption of permutation invariance states that all emitters are equal in their dynamics and interaction between any pair of emitters is the same. In cases of ion channels which gate cooperatively as a consequence of chemical interaction between nearby channels, this assumption is violated. The requirement of conditional independence goes even further and restricts interaction between emitters to stem exclusively from the overall state of the system which leads to a “mean field like” interaction.

In the case of ion channels, the measured signal is usually filtered by a Bessel filter, which leads to dependency of the data. We disregard filtering here, which leads to systematic errors on short time scales. In consequence, the Viterbi algorithm, which aims to determine the underlying Markov state at each time point, produces flawed results on very short time scales. Especially a transition from state 0 to state 2 or vice versa can easily be mistaken for two transitions, from state 0 to 1 and from 1 to 2. This can distort the resulting estimated transition matrix.

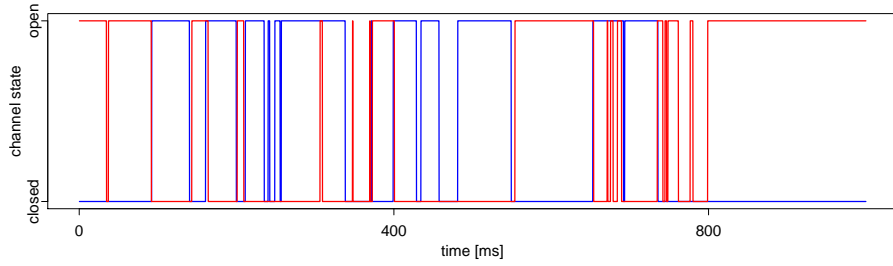
In the application to RyR2 channels which we present, we find clear evidence for strong competitive gating. To our knowledge, this is the first time such behavior has been described for ion channels. While far-reaching biochemical conclusions cannot be drawn from this finding, this calls for further experimental investigation to check whether this result can be compounded, how it can be explained and whether it has biochemical implications.

### **Acknowledgements**

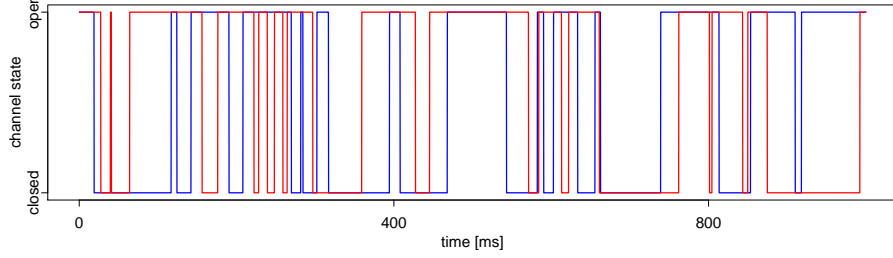
The authors acknowledge support of the DFG SFB 803 project Z02 and the DFG Cluster of Excellence 2067 MBExC. The data set was provided by Lehnart's Lab from the Cellular Biophysics and Translational Cardiology Section in the Heart Research Center Göttingen (HRCG). S. E. Lehnart was supported by Deutsche Forschungsgemeinschaft SPP1926 Next Generation Optogenetics.

## A Illustration to Section 1

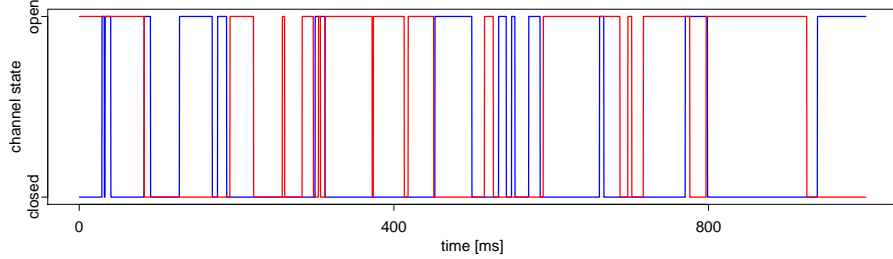
Figure 5 below contains a decomposition of measured data into possible marginal traces of two individual channels, displayed in red and blue. For simplicity, events are excluded in which one channel opens and the other closes at exactly the same time. Instead, for every time interval, during which the measured sum process remains in state 1, indicating one open channel, one of the two channels is chosen to be open at random. The resulting possible traces are compared to marginal traces simulated from CK and VND models using estimated model parameters. Clearly, the possible data traces resemble much more closely the VND traces than the CK traces. While the CK traces are uncorrelated, the VND traces as well as the possible traces for real data show very strong negative correlation.



(a) *data set 1*



(b) *CK model with  $\hat{\kappa} = 0$*



(c) *VND model*

Figure 5: *Decomposition of measured data into possible marginal traces of two individual channels, displayed in red and blue.*

## B Proofs of Section 2

### B.1 Proof of Lemma 2.2

First we show that the lumping property implies (6). We have

$$\begin{aligned}
\mathbb{P}(S_{k+1} = j \mid S_k = m) &= \sum_{z \in \mathcal{Z}_m} \frac{\mathbb{P}(S_{k+1} = j, S_k = m, X_k = z)}{\mathbb{P}(S_k = m)} \\
&= \sum_{z \in \mathcal{Z}_m} \frac{\mathbb{P}(S_{k+1} = j, X_k = z)}{\mathbb{P}(X_k = z)} \frac{\mathbb{P}(X_k = z)}{\mathbb{P}(S_k = m)} \\
&= \mathbb{P}(S_{k+1} = j \mid X_k = x) \frac{1}{\mathbb{P}(S_k = m)} \sum_{z \in \mathcal{Z}_m} \mathbb{P}(X_k = z) \\
&= \mathbb{P}(S_{k+1} = j \mid X_k = x),
\end{aligned}$$

where we used the lumping property in the second last equality. The other direction is obvious, since in the right-hand side of (6) we can substitute  $x$  by any  $y \in \mathcal{Z}_m$ .

### B.2 Proof of Proposition 2.3

We verify the Markov property. For  $k \in \mathbb{N}$  and arbitrary  $i_1, \dots, i_{k+1} \in [\ell]$  we have

$$\begin{aligned}
&\mathbb{P}(S_{k+1} = i_{k+1} \mid S_k = i_k, \dots, S_1 = i_1) \cdot \mathbb{P}(S_k = i_k, \dots, S_1 = i_1) \\
&= \sum_{x_1 \in \mathcal{Z}_{i_1}} \cdots \sum_{x_{k+1} \in \mathcal{Z}_{i_{k+1}}} \mathbb{P}(S_{k+1} = i_{k+1}, X_{k+1} = x_{k+1}, S_k = i_k, X_k = x_k, \dots, S_1 = i_1, X_1 = x_1) \\
&= \sum_{x_1 \in \mathcal{Z}_{i_1}} \cdots \sum_{x_{k+1} \in \mathcal{Z}_{i_{k+1}}} \mathbb{P}(X_{k+1} = x_{k+1}, X_k = x_k, \dots, X_1 = x_1) \\
&= \sum_{x_1 \in \mathcal{Z}_{i_1}} \cdots \sum_{x_{k+1} \in \mathcal{Z}_{i_{k+1}}} \mathbb{P}(X_{k+1} = x_{k+1} \mid X_k = x_k) \mathbb{P}(X_k = x_k, \dots, X_1 = x_1). \quad (17)
\end{aligned}$$

Here in the last equality we used the Markov property of the Markov chain  $(X_k)_{k \in \mathbb{N}_0}$ . For  $x_k \in \mathcal{Z}_{i_k}$  we have by Lemma 2.2

$$\begin{aligned}
\sum_{x_{k+1} \in \mathcal{Z}_{i_{k+1}}} \mathbb{P}(X_{k+1} = x_{k+1} \mid X_k = x_k) &= \mathbb{P}(S_{k+1} = i_{k+1} \mid X_k = x_k) \\
&= \mathbb{P}(S_{k+1} = i_{k+1} \mid S_k = i_k).
\end{aligned}$$

By plugging this in (17) and the fact that

$$\mathbb{P}(S_k = i_k, \dots, S_1 = i_1) = \sum_{x_1 \in \mathcal{Z}_{i_1}} \cdots \sum_{x_k \in \mathcal{Z}_{i_k}} \mathbb{P}(X_k = x_k, \dots, X_1 = x_1)$$

the assertion is proven.

### B.3 Proof of Proposition 2.7

Let  $i, j \in [\ell]$  and  $x, x' \in \mathcal{Z}_i$ . Note that  $x, x' \in \mathcal{Z}_i$  implies that the vectors  $x, x'$  have the same number of “1” entries and therefore, there exists a permutation matrix  $P \in \{0, 1\}^{\ell \times \ell}$  such that  $Px = x'$ . Then

$$\begin{aligned} \mathbb{P}(S_{k+1} = j \mid X_k = x) &= \sum_{y \in \mathcal{Z}_j} \mathbb{P}(X_{k+1} = y \mid X_k = x) \\ &= \sum_{y \in \mathcal{Z}_j} \mathbb{P}(X_{k+1} = Py \mid X_k = Px) \\ &= \sum_{y \in \mathcal{Z}_j} \mathbb{P}(X_{k+1} = y \mid X_k = x') = \mathbb{P}(S_{k+1} = j \mid X_k = x'). \end{aligned}$$

### B.4 Proof of Lemma 2.8

For  $x, y \in \{0, 1\}^\ell$  define the  $\{0, 1\}^2$ -valued vector

$$\mathbf{z}_{x,y} := (x, y)^T = ((x^{(1)}, y^{(1)}), \dots, (x^{(\ell)}, y^{(\ell)}))^T.$$

Then, there exists a permutation matrix  $P_{x,y} \in \{0, 1\}^{\ell \times \ell}$  with  $n^{(1)}, \dots, n^{(4)} \in [\ell]$  and  $\sum_{i=1}^4 n^{(i)} = \ell$  such that the entries of  $P_{x,y} \mathbf{z}_{x,y}$  satisfy

$$(P_{x,y} \mathbf{z}_{x,y})^{(i)} = \begin{cases} (0, 0) & 1 \leq i \leq n^{(1)} \\ (0, 1) & 1 + n^{(1)} \leq i \leq n^{(1)} + n^{(2)} \\ (1, 0) & 1 + n^{(1)} + n^{(2)} \leq i \leq \sum_{j=1}^3 n^{(j)} \\ (1, 1) & 1 + \sum_{j=1}^3 n^{(j)} \leq i \leq \ell. \end{cases}$$

Note that the permutation  $P_{x,y}$  orders the pairs within the vector  $\mathbf{z}_{x,y}$  according to the lexicographic semioorder.

For the given  $x_1, y_1, x_2, y_2 \in \{0, 1\}^\ell$  satisfying (9) we consider the permutation matrices  $P_{x_1, y_1}$  with the numbers  $n_1^{(j)} \in [\ell]$  for  $j = 1, \dots, 4$  and  $P_{x_2, y_2}$  with  $n_2^{(j)} \in [\ell]$ , such that  $\sum_{j=1}^4 n_i^{(j)} = \ell$  for  $i = 1, 2$ . Observe that if we are able to verify that  $P_{x_1, y_1} \mathbf{z}_{x_1, y_1} = P_{x_2, y_2} \mathbf{z}_{x_2, y_2}$ , then (10) follows with

$$P = P_{x_1, y_1}^{-1} P_{x_2, y_2}.$$

Therefore, to prove the statement of (10) it is sufficient to show that  $n_1^{(j)} = n_2^{(j)}$  for  $j = 1, \dots, 4$ . For this note that (9) implies

$$\begin{aligned} n_1^{(1)} + n_1^{(2)} &= \ell - \|x_1\|_1 = \ell - \|x_2\|_1 = n_2^{(1)} + n_2^{(2)} \\ n_1^{(1)} + n_1^{(3)} &= \ell - \|y_1\|_1 = \ell - \|y_2\|_1 = n_2^{(1)} + n_2^{(3)} \\ n_1^{(1)} + n_1^{(4)} &= \ell - \|x_1 - y_1\|_1 = \ell - \|x_2 - y_2\|_1 = n_2^{(1)} + n_2^{(4)}. \end{aligned}$$

Having those three equations and using  $\sum_{i=1}^4 n_1^{(i)} = \sum_{i=1}^4 n_2^{(i)} = \ell$  yields to the desired fact that  $n_1^{(j)} = n_2^{(j)}$  for  $j = 1, \dots, 4$ .

As a consequence with the invariance property for  $k \in \mathbb{N}_0$  we get

$$\mathbb{P}(X_{k+1} = y_1 \mid X_k = x_1) \stackrel{(10)}{=} \mathbb{P}(X_{k+1} = Py_2 \mid X_k = Px_2) = \mathbb{P}(X_{k+1} = y_2 \mid X_k = x_2),$$

which finishes the proof.

## B.5 Proof of Proposition 2.9

For  $j, k \in [\ell]$  define

$$n_{j,k} := |\{ \|x - y\|_1 : x \in \mathcal{Z}_j, y \in \mathcal{Z}_k \}|,$$

which denotes the number of different possible values of the sum of “1”s within the difference of vectors with  $j$  and  $k$  non-zero entries. For  $x, y \in \{0, 1\}^\ell$  with  $x \in \mathcal{Z}_j$  and  $y \in \mathcal{Z}_k$  it is clear that switching all “0” and “1” entries in  $x$  and  $y$  does not change  $\|x - y\|_1$ , such that  $n_{j,k} = n_{\ell-j, \ell-k}$ . Similarly one can conclude that

$$n_{j,k} = n_{\ell-j, k} = n_{j, \ell-k}.$$

Furthermore,  $n_{j,k} = n_{k,j}$ , because  $\|x - y\|_1$  is symmetric under interchange of  $x$  and  $y$ . For  $j \leq k \leq \frac{\ell-1}{2}$  we obtain

$$n_{j,k} = |\{0, 1, \dots, j\}| = j + 1,$$

and taking the symmetries explained above into account we get for any  $j, k \in [\ell]$  that

$$n_{j,k} = \min\{j + 1, k + 1, \ell + 1 - j, \ell + 1 - k\}.$$

Thus, by Lemma 2.8 the number  $N_{\text{PI}}$  of (possibly) different transition matrix entries for a permutation invariant Markov chain is

$$\begin{aligned} N_{\text{PI}}(\ell) &= \sum_{j=0}^{\ell} \sum_{k=0}^{\ell} \min\{j + 1, k + 1, \ell + 1 - j, \ell + 1 - k\} \\ &= (\ell + 1)(\ell + 2)(\ell + 3)/6. \end{aligned}$$

The latter equality is shown by induction using the middle-split

$$\begin{aligned} N_{\text{PI}}(\ell + 1) &= \sum_{\substack{j=0 \\ j \neq \lfloor \frac{\ell}{2} + 1 \rfloor}}^{\ell+1} \sum_{\substack{k=0 \\ k \neq \lfloor \frac{\ell}{2} + 1 \rfloor}}^{\ell+1} \min\{j + 1, k + 1, \ell + 2 - j, \ell + 2 - k\} + \frac{(\ell + 2)(\ell + 3)}{2} \\ &= \sum_{j=0}^{\ell} \sum_{k=0}^{\ell} \min\{j + 1, k + 1, \ell + 1 - j, \ell + 1 - k\} + \frac{(\ell + 2)(\ell + 3)}{2} \\ &= N_{\text{PI}}(\ell) + \frac{(\ell + 2)(\ell + 3)}{2}, \end{aligned}$$

which yields the result. The number of independent entries/parameters in the transition matrix is further reduced, since all rows of the matrix sum up to one. The first entry in every row can therefore be considered dependent on the other entries in the row. As there are  $\ell + 1$  independent parameters in the first column, the total number of independent parameters is

$$(\ell + 1)(\ell + 2)(\ell + 3)/6 - 6(\ell + 1)/6 = \ell(\ell + 1)(\ell + 5)/6.$$

## B.6 Proof of Lemma 2.17

For the proof of this lemma we require the following auxiliary results:

**Lemma B.1.** *Let  $A, B_1, \dots, B_k \in \mathcal{F}$  with pairwise disjoint  $B_1, \dots, B_k$ . Assume that  $\mathbb{P}(B_i) = \mathbb{P}(B_j)$  and  $\mathbb{P}(A | B_i) = \mathbb{P}(A | B_j)$  for all  $i, j \in \{1, \dots, k\}$ . Then*

$$\mathbb{P}\left(A \mid \bigsqcup_{j=1}^k B_j\right) = \mathbb{P}(A | B_i)$$

for all  $i \in \{1, \dots, k\}$ . (Here  $\bigsqcup$  denotes a union of pairwise disjoint sets.)

*Proof.* It is sufficient to show the statement for  $k = 2$ , since then the rest follows inductively. For  $k = 2$  we have

$$\begin{aligned} \mathbb{P}(A | B_1 \sqcup B_2) &= \frac{\mathbb{P}(A \cap (B_1 \sqcup B_2))}{\mathbb{P}(B_1 \sqcup B_2)} = \frac{\mathbb{P}((A \cap B_1) \sqcup (A \cap B_2))}{\mathbb{P}(B_1 \sqcup B_2)} \\ &= \frac{\mathbb{P}(A \cap B_1) + \mathbb{P}(A \cap B_2)}{2\mathbb{P}(B_1)} = \frac{\mathbb{P}(A \cap B_1)}{2\mathbb{P}(B_1)} + \frac{\mathbb{P}(A \cap B_2)}{2\mathbb{P}(B_2)} \\ &= (1/2)\mathbb{P}(A | B_1) + (1/2)\mathbb{P}(A | B_2) \\ &= \mathbb{P}(A | B_1) = \mathbb{P}(A | B_2). \end{aligned}$$

□

□

**Lemma B.2.** *Let  $(X_k)_{k \in \mathbb{N}_0}$  be a permutation invariant vector Markov chain with*

$$\mathbb{P}(X_0 = y) = \mathbb{P}(X_0 = Py), \quad y \in \{0, 1\}^\ell,$$

for a permutation matrix  $P \in \{0, 1\}^{\ell \times \ell}$ . Then, for any  $k \in \mathbb{N}_0$  we have

$$\mathbb{P}(X_k = y) = \mathbb{P}(X_k = Py), \quad y \in \{0, 1\}^\ell. \quad (18)$$

*Proof.* We prove the statement by induction over  $k$ . Note that, by assumption, (18) holds for  $k = 0$ . If it is true for  $k$ , then

$$\begin{aligned} \mathbb{P}(X_{k+1} = y) &= \sum_{x \in \{0, 1\}^\ell} \mathbb{P}(X_{k+1} = y | X_k = x) \mathbb{P}(X_k = x) \\ &= \sum_{x \in \{0, 1\}^\ell} \mathbb{P}(X_{k+1} = Py | X_k = Px) \mathbb{P}(X_k = Px) \\ &= \mathbb{P}(X_{k+1} = Py), \end{aligned}$$

which verifies (18) for  $k + 1$  and finishes the proof. □

Now we prove Lemma 2.17:

*Proof.* Define the set

$$I_{x,i} := \{z \in \mathcal{Z}_{\|x\|_1} \mid x^{(i)} = z^{(i)}\}.$$

We aim to apply Lemma B.1 with  $A = \{X_{k+1}^{(i)} = y^{(i)}\}$  and  $B_z = \{X_k = z\}$  for  $z \in I_{x,i}$ . For any  $z \in I_{x,i}$  we have a permutation matrix  $P$  such that  $Px = z$  and  $(Pz')^{(i)} = z'^{(i)}$  for any  $z' \in \{0, 1\}^\ell$ . (The last condition says that the permutation does not change the  $i$ th coordinate entry.) Then, with Lemma B.2 we have

$$\mathbb{P}(B_x) = \mathbb{P}(X_k = x) = \mathbb{P}(X_k = Px) = \mathbb{P}(B_z).$$

In addition to that, by the permutation invariance we obtain

$$\begin{aligned} \mathbb{P}(A \mid B_x) &= \mathbb{P}(X_{k+1}^{(i)} = y^{(i)} \mid X_k = x) = \mathbb{P}(X_{k+1}^{(i)} = (Py)^{(i)} \mid X_k = Px) \\ &= \mathbb{P}(X_{k+1}^{(i)} = y^{(i)} \mid X_k = z) = \mathbb{P}(A \mid B_z). \end{aligned}$$

Furthermore

$$\bigsqcup_{z \in I_{x,i}} B_z = \bigsqcup_{z \in I_{x,i}} \{X_k = z\} = \{X_k^{(i)} = x^{(i)}, \|X_k\|_1 = \|x\|_1\}.$$

Thus, by the application of Lemma B.1 we have (14).  $\square$

## B.7 Proof of Proposition 2.19

For arbitrary  $i \in [\ell]$  set

$$x = (\underbrace{1, \dots, 1}_{i \text{ times}}, \underbrace{0, \dots, 0}_{\ell-i \text{ times}})$$

and note that  $x \in \mathcal{Z}_i$ . Thus, for  $j \in [\ell]$  by the lumping property we have

$$q_{i,j} = \mathbb{P}(S_{k+1} = j \mid X_k = x).$$

The idea is to decompose the event  $X_k = x$  into different sets in such a way that we can use counting problem arguments. For this define the random variable

$$R := \text{“The number of 1s from } x \text{ that become 0s at time } k+1\text{”}.$$

Observe that the random variable  $R$  takes only values in  $\{\max\{0, i-j\}, \dots, \min\{i, \ell-j\}\}$ , since trivially  $0 \leq R \leq i$ ,  $R \geq i-j$  because the number of ones at time  $k+1$  is  $j$  and  $R \leq \ell-j$  follows by the fact that the number of zeros at time  $k+1$  is  $\ell-j$ . Furthermore, we have

$$q_{i,j} = \sum_{r=\max\{0, i-j\}}^{\min\{i, \ell-j\}} \mathbb{P}(S_{k+1} = j, R = r \mid X_k = x).$$



For  $r \in \{\max\{0, i - j\}, \dots, \min\{i, \ell - j\}\}$  we have

$$\mathbb{P}(S_{k+1} = j, R = r \mid X_k = x) = \binom{i}{r} \binom{\ell - i}{j - i + r} \eta_i^{i-r} (1 - \eta_i)^r \lambda_i^{\ell-j-r} (1 - \lambda_i)^{j-i+r}, \quad (19)$$

which is justified as follows. Recall that  $R = r$  means that there were  $r$  ones that became zeros and observe that the number of cases when that happens is  $\binom{i}{r} \binom{\ell-i}{j-i+r}$ . (This is true since there are  $\binom{i}{r}$  possibilities for  $r$  ones to become zeros and eventually, to have  $j$  ones at time  $k+1$ , there are  $\binom{\ell-i}{j-i+r}$  possibilities of zeros which become ones.) Finally, by taking into account that the probabilities of  $i-r$  ones to remain ones is  $\eta_i^{i-r}$ , of  $r$  ones to become zeros is  $(1 - \eta_i)^r$ , of  $j - i + r$  zeros to become ones is  $(1 - \lambda_i)^{j-i+r}$  and of  $\ell - j - r$  zeros to remain zeros is  $\lambda_i^{\ell-j-r}$ , the representation of (19) is verified.

## B.8 Proof of Theorem 1.5

In Proposition 2.19 we provided a functional representation of the entries of  $Q = (q_{s,r})_{s,r \in [\ell]}$  in terms of the parameters  $\lambda_0, \dots, \lambda_{\ell-1}, \eta_1, \dots, \eta_\ell \in [0, 1]$ . The idea is to exploit this structure.

First, observe that  $q_{0,0} = \lambda_0^\ell$  and  $q_{\ell,\ell} = \eta_\ell^\ell$  such that  $\lambda_0$  and  $\eta_\ell$  are uniquely determined. If  $\ell = 1$ , this concludes the proof, so that in all of the following we can assume  $\ell \geq 2$ . For  $i = 1, 2$  let  $\lambda_{0,(i)}, \dots, \lambda_{\ell-1,(i)}, \eta_{1,(i)}, \dots, \eta_{\ell,(i)} \in [0, 1]$  be solutions of the inverse lumping problem (of course with  $\lambda_{0,(i)} = q_{0,0}^{1/\ell}$  and  $\eta_{\ell,(i)} = q_{\ell,\ell}^{1/\ell}$ ). For  $s \in \{1, \dots, \ell - 1\}$  let us use the notation  $\tilde{\eta}_{s,(i)} := 1 - \eta_{s,(i)}$  and note that from Proposition 2.19 it follows that

$$\tilde{\eta}_{s,(1)}^s \lambda_{s,(1)}^{\ell-s} = q_{s,0} = \tilde{\eta}_{s,(2)}^s \lambda_{s,(2)}^{\ell-s}. \quad (20)$$

We immediately see that  $\tilde{\eta}_{s,(1)} = \tilde{\eta}_{s,(2)}$  iff  $\lambda_{s,(1)} = \lambda_{s,(2)}$ . Now, for  $s \in \{1, \dots, \ell - 1\}$  assume that the pair  $(\tilde{\eta}_{s,(1)}, \lambda_{s,(1)})$  is different from  $(\tilde{\eta}_{s,(2)}, \lambda_{s,(2)})$ , which leads to the fact that without loss of generality we have  $\lambda_{s,(1)} > 0$ . Therefore  $x := \lambda_{s,(2)}/\lambda_{s,(1)} \in [0, \infty)$ . Additionally by  $s \in \{1, \dots, \ell - 1\}$  we have  $\alpha := \ell/s \in (1, \ell]$ . By exploiting (20) we obtain  $\tilde{\eta}_{s,(2)} = \tilde{\eta}_{s,(1)} x^{1-\alpha}$  and trivially  $\lambda_{s,(2)} = \lambda_{s,(1)} x$ , which gives

$$x - \tilde{\eta}_{s,(2)} x = (x^\alpha - \tilde{\eta}_{s,(1)} x) x^{1-\alpha}, \quad (21)$$

$$x - \lambda_{s,(2)} x = (1 - \lambda_{s,(1)} x) x. \quad (22)$$

Taking the form of  $q_{s,1}$  from Proposition 2.19 into account yields

$$\begin{aligned} s \tilde{\eta}_{s,(1)}^{s-1} (x - \tilde{\eta}_{s,(1)} x) \lambda_{s,(1)}^{\ell-s} + (\ell - s) \tilde{\eta}_{s,(1)}^s \lambda_{s,(1)}^{\ell-s-1} (x - \lambda_{s,(1)} x) &= x q_{s,1} \\ &= s \tilde{\eta}_{s,(2)}^{s-1} (x - \tilde{\eta}_{s,(2)} x) \lambda_{s,(2)}^{\ell-s} + (\ell - s) \tilde{\eta}_{s,(2)}^s \lambda_{s,(2)}^{\ell-s-1} (x - \lambda_{s,(2)} x). \end{aligned}$$

Using (21) and (22) on the left-hand side of the previous equality gives

$$\begin{aligned} s \tilde{\eta}_{s,(1)}^{s-1} (x - \tilde{\eta}_{s,(1)} x) \lambda_{s,(1)}^{\ell-s} + (\ell - s) \tilde{\eta}_{s,(1)}^s \lambda_{s,(1)}^{\ell-s-1} (x - \lambda_{s,(1)} x) \\ = s \tilde{\eta}_{s,(1)}^{s-1} (x^\alpha - \tilde{\eta}_{s,(1)} x) \lambda_{s,(1)}^{\ell-s} + (\ell - s) \tilde{\eta}_{s,(1)}^s \lambda_{s,(1)}^{\ell-s-1} (1 - \lambda_{s,(1)} x). \end{aligned}$$

Further transformations of this yield

$$x^\alpha = x + \frac{\ell - s}{s} \frac{\tilde{\eta}_{s,(1)}}{\lambda_{s,(1)}} (x - 1). \quad (23)$$

It is clear that  $x = 1$  is a solution to equation (23) and that there is at most one other solution. To find a simple expression for the other solution for general  $\alpha$ , we consider the representation of  $q_{s,2}$  (again) from Proposition 2.19. We have

$$\begin{aligned} & s(s-1)\tilde{\eta}_{s,(1)}^{s-2}(x - \tilde{\eta}_{s,(1)}x)^2\lambda_{s,(1)}^{\ell-s} \\ & + 2s(\ell-s)\tilde{\eta}_{s,(1)}^{s-1}\lambda_{s,(1)}^{\ell-s-1}(x - \tilde{\eta}_{s,(1)}x)(x - \lambda_{s,(1)}x) \\ & + (\ell-s)(\ell-s-1)\tilde{\eta}_{s,(1)}^s\lambda_{s,(1)}^{\ell-s-2}(x - \lambda_{s,(1)}x)^2 = 2x^2q_{s,2} \\ & = s(s-1)\tilde{\eta}_{s,(2)}^{s-2}(x - \tilde{\eta}_{s,(2)}x)^2\lambda_{s,(2)}^{\ell-s} \\ & + 2s(\ell-s)\tilde{\eta}_{s,(2)}^{s-1}\lambda_{s,(2)}^{\ell-s-1}(x - \tilde{\eta}_{s,(2)}x)(x - \lambda_{s,(2)}x) \\ & + (\ell-s)(\ell-s-1)\tilde{\eta}_{s,(2)}^s\lambda_{s,(2)}^{\ell-s-2}(x - \lambda_{s,(2)}x)^2. \end{aligned}$$

Note that in the special case  $s = 1$  the first term on either side vanishes and the remaining terms are exactly those given in Proposition 2.19. By (21) and (22) the right-hand side can be further modified such that

$$\begin{aligned} & s(s-1)\tilde{\eta}_{s,(1)}^{s-2}(x - \tilde{\eta}_{s,(1)}x)^2\lambda_{s,(1)}^{\ell-s} \\ & + 2s(\ell-s)\tilde{\eta}_{s,(1)}^{s-1}\lambda_{s,(1)}^{\ell-s-1}(x - \tilde{\eta}_{s,(1)}x)(x - \lambda_{s,(1)}x) \\ & + (\ell-s)(\ell-s-1)\tilde{\eta}_{s,(1)}^s\lambda_{s,(1)}^{\ell-s-2}(x - \lambda_{s,(1)}x)^2 \\ & = s(s-1)\tilde{\eta}_{s,(1)}^{s-2}(x^\alpha - \tilde{\eta}_{s,(1)}x)^2\lambda_{s,(1)}^{\ell-s} \\ & + 2s(\ell-s)\tilde{\eta}_{s,(1)}^{s-1}\lambda_{s,(1)}^{\ell-s-1}(x^\alpha - \tilde{\eta}_{s,(1)}x)(1 - \lambda_{s,(1)}x) \\ & + (\ell-s)(\ell-s-1)\tilde{\eta}_{s,(1)}^s\lambda_{s,(1)}^{\ell-s-2}(1 - \lambda_{s,(1)}x)^2. \end{aligned}$$

By plugging (23) in, the previous expression reduces to a quadratic equation in  $x$ . One solution is again  $x = 1$  and the other solution is

$$x = \frac{\ell\tilde{\eta}_{s,(1)}}{\ell\tilde{\eta}_{s,(1)} - 2s\tilde{\eta}_{s,(1)} + 2s\lambda_{s,(1)}} = \frac{\alpha\tilde{\eta}_{s,(1)}}{(\alpha-2)\tilde{\eta}_{s,(1)} + 2\lambda_{s,(1)}}.$$

Defining  $y := \frac{\lambda_{s,(1)}}{\tilde{\eta}_{s,(1)}}$ , we obtain  $x = \frac{\alpha}{2y + \alpha - 2}$  and from  $x \in [0, \infty)$  we get  $y \in (1 - \frac{\alpha}{2}, \infty]$ . Substituting the second solution back into equation (23) yields

$$\left(\frac{\alpha}{2y + \alpha - 2}\right)^\alpha = \frac{1}{y} \frac{(2\alpha - 2) - (\alpha - 2)y}{2y + \alpha - 2} \quad (24)$$

which can be rewritten as

$$f_\alpha(y) := (2y + \alpha - 2)^{\alpha-1}((\alpha - 2)y - 2(\alpha - 1)) + \alpha^\alpha y = 0.$$

Note that  $f_\alpha$  is continuous on the whole domain for every  $\alpha > 1$ . Straightforward calculations give

$$\begin{aligned} f'_\alpha(y) &= \alpha(2y + \alpha - 2)^{\alpha-2}(2(\alpha - 2)y - 3\alpha + 4) + \alpha^\alpha, \\ f''_\alpha(y) &= 4\alpha(\alpha - 1)(\alpha - 2)(2y + \alpha - 2)^{\alpha-3}(y - 1), \\ f'''_\alpha(y) &= 4\alpha(\alpha - 1)(\alpha - 2)(2y + \alpha - 2)^{\alpha-4}(2(\alpha - 2)y - \alpha + 4), \\ f'''_\alpha(1) &= 4\alpha^{\alpha-2}(\alpha - 1)(\alpha - 2), \\ g_\alpha(\epsilon) &:= f'_\alpha\left(1 - \frac{\alpha}{2} + \epsilon\right) = -\alpha^2(\alpha - 1)\epsilon^{\alpha-2} - 2\alpha^2(2 - \alpha)\epsilon^{\alpha-1} + \alpha^\alpha. \end{aligned}$$

We treat three cases:

**Case 1:**  $\alpha > 2$

Here,  $1 - \alpha/2 < 0$  and thus  $y \geq 0$ . We have  $f''_\alpha(y) = 0$  if and only if  $y = 1$  and  $f'''_\alpha(1) > 0$ , so  $f'_\alpha(y)$  has a unique global minimum at  $y = 1$ . Since  $f'_\alpha(1) = 0$  this means that  $f'_\alpha(y) > 0$  for all  $y > 0$ . Since  $f_\alpha(1) = 0$  and  $\lim_{y \rightarrow \infty} f_\alpha(y) = \infty$ , we conclude that  $y = 1$  is the only zero.

**Case 2:**  $\alpha = 2$

Note that this case only occurs if  $\ell$  is even. Here,  $f_2(y) = 0$  for any  $y > 0$  and we have

$$x = \frac{1}{y} \iff \frac{\lambda_{s,(2)}}{\lambda_{s,(1)}} = \frac{\tilde{\eta}_{s,(1)}}{\lambda_{s,(1)}} \iff \lambda_{s,(2)} = \tilde{\eta}_{s,(1)} \iff \lambda_{s,(1)} = \tilde{\eta}_{s,(2)}.$$

If  $\lambda_{s,(1)} \geq \tilde{\eta}_{s,(1)}$ , we get  $\lambda_{s,(2)} = \tilde{\eta}_{s,(1)} \leq \lambda_{s,(1)} = \tilde{\eta}_{s,(2)}$  which means that the second solution is invalid unless both solutions are the same, which is excluded by assumption. Thus only one of the solutions is valid.

**Case 3:**  $1 < \alpha < 2$

Here,  $1 - \alpha/2 > 0$  and thus  $y > 1 - \alpha/2$ . We have  $f''_\alpha(y) = 0$  if and only if  $y = 1$  and  $f'''_\alpha(1) < 0$ , so  $f'_\alpha(y)$  has a local maximum at  $y = 1$ . For completeness, we notice

$$\lim_{y \searrow 1 - \frac{\alpha}{2}} f'_\alpha(y) = \lim_{\epsilon \searrow 0} g_\alpha(\epsilon) = \lim_{\epsilon \searrow 0} (-\alpha^2(\alpha - 1)\epsilon^{\alpha-2} - 2\alpha^2(2 - \alpha)\epsilon^{\alpha-1} + \alpha^\alpha) = -\infty.$$

This means that  $f'_\alpha(y) < 0$  for  $y > 1 - \alpha/2$ . Since  $f_\alpha(1) = 0$ , we conclude that  $f_\alpha(y) < 0$  for  $y > 1$  and  $f_\alpha(y) > 0$  for  $1 - \frac{\alpha}{2} < y < 1$ . Furthermore, note that

$$\lim_{y \rightarrow \infty} f_\alpha(y) = \lim_{y \rightarrow \infty} ((\alpha - 2)2^{\alpha-1}y^\alpha + \alpha^\alpha y) = (\alpha - 2)2^{\alpha-1} \lim_{y \rightarrow \infty} y^\alpha = -\infty$$

thus we conclude that  $y = 1$  is the only zero.

This proves the claim of uniqueness since in all three cases we obtain  $\lambda_{s,(1)} = \lambda_{s,(2)}$  and therefore  $\eta_{s,(1)} = \eta_{s,(1)}$  which contradicts the assumption that the tuples  $(\lambda_{s,(i)}, \eta_{s,(i)})$  with  $i = 1, 2$  are different to each other.

## C Illustration to Section 3

We consider the case of  $\ell = 2$  and use the polynomials

$$P_0(\theta_H) = \sum_{i=0}^2 n_{0,i} \log q_{0,i}^{(\text{VND})}(\lambda_0), \quad (25)$$

$$P_1(\theta_H) = \sum_{i=0}^2 n_{1,i} \log q_{1,i}^{(\text{VND})}(\lambda_1, \eta_1), \quad (26)$$

$$P_2(\theta_H) = \sum_{i=0}^2 n_{2,i} \log q_{2,i}^{(\text{VND})}(\eta_2), \quad (27)$$

where the number of state changes from  $i$  to  $j$  in  $S_{1:K}$  is denoted as  $n_{i,j}$ . With that we have  $\sum_{k=0}^2 P_k(\theta_H) = \sum_{k=1}^{K-1} \log q_{s_k, s_{k+1}}^{(\text{VND})}(\theta_H)$ , which provides a representation of the “middle” term of the log-likelihood function

$$\ell(\theta, s_{1:K}, y_{1:K}) = \log \pi^{(s_1)} + \sum_{k=1}^{K-1} \log q_{s_k, s_{k+1}}^{(\text{VND})}(\theta_H) + \sum_{k=1}^K \log g_{\theta_E}(y_k, s_k). \quad (28)$$

This log-likelihood function is fundamental for the Baum-Welch algorithm, in particular it leads to  $\theta \mapsto f(\theta, \theta_t, y_{1:K})$  which is the function that is used in the maximization step, described in Section 3.2 of the main text. From (28) we obtain that for unimodality of  $\theta \mapsto f(\theta, \theta_t, y_{1:K})$  it is sufficient to show that  $\sum_{k=0}^2 P_k(\theta_H)$  is strictly unimodal, since the two other terms are strictly concave in the Gaussian scenario we are interested in. Therefore, in Figure 6 we plot  $P_0$ ,  $P_1$  and  $P_2$  to provide an indication of their behavior. In general  $\sum_{k=0}^2 P_k(\theta_H)$  is not strictly unimodal, but a sufficient condition may be to restrict to  $\lambda_1 \geq 1 - \eta_1$ .

## D Details to Section 4

### D.1 Planar lipid bilayer channel measurements

ER vesicles from HEK293 cells expressing RyR2-WT were prepared as described previously (Meli et al., 2011). Planar lipid bilayers were formed by painting a mixture of phosphatidylethanolamine and phosphatidylcholine (3:1 ratio; Avanti Polar Lipids) across 200- $\mu\text{m}$  aperture in polysulfonate cup (Warner Instruments) separating 2 chambers. The trans chamber (1.0 ml), representing the intra-SR (luminal) compartment, was connected to the head stage input of a bilayer voltage clamp amplifier. The cis chamber (1.0 ml), representing the cytoplasmic compartment, was held at virtual ground. Used basic solutions were as follows: 1 mM EGTA, 250/125 mM Hepes/Tris, 50 mM KCl, 0.64 mM  $\text{CaCl}_2$ , pH 7.35 as cis solution (150 nM free  $[\text{Ca}^{2+}]$ ) and 53 mM  $\text{Ba}(\text{OH})_2$ , 50 mM KCl, 250 mM Hepes, pH 7.35 as trans solution. RyR2-WT channels were reconstituted by spontaneously fusing ER vesicles into the planar lipid bilayer. Currents through incorporated

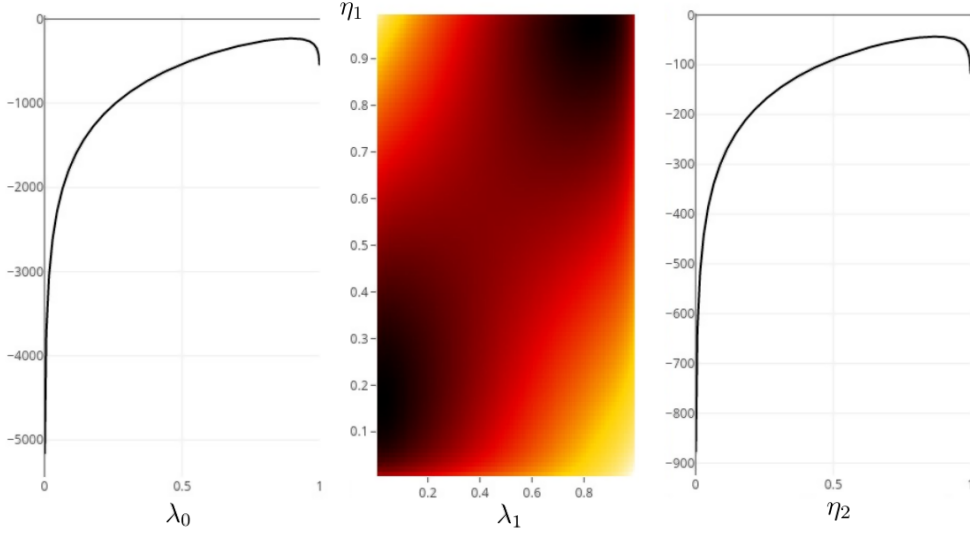


Figure 6: From a simulation of 1000 points from the VND model with parameters  $(0.9, 0.8, 0.98, 0.89)$  plots of the polynomials  $P_0$  (25),  $P_1$  (26), and  $P_2$  (27) respectively. The plot of  $P_1$  is depicted here as a heat map. Although, this heat map shows two maxima (in black), if one restricts to  $\lambda_1 \geq 1 - \eta_1$  the resulting polynomial is strictly unimodal.

RyR2-WT channels were recorded at 0 mV using an amplifier (BC-525D, Warner Instruments), filtered at 1 kHz (LPF-8, Warner Instruments), and digitized at 4 kHz. Data acquisition was performed using Digidata 1440A and Axoscope 10 software (Axon Instruments). Activity / gating of RyR2-WT channels was first recorded at 150 nM cytosolic  $[\text{Ca}^{2+}]$  and either 5 or 10 mM luminal  $[\text{Ca}^{2+}]$ . After that, the cytosolic  $[\text{Ca}^{2+}]$  was increased up to 5  $\mu\text{M}$  together with addition of 1mM Na-ATP to fully activate and to assess the number of channels in bilayer. At the end of the experiment, 8-16  $\mu\text{M}$  ryanodine was applied to confirm RyR2 channels identity.

## D.2 Estimating the number of channels

After we have established the VND model to provide a reasonable fit to the data, we would like to determine the true number of channels. From an experiment adding a high concentration of ATP to the system, we have the direct estimate that the number of channels is approximately  $\ell \approx 20$ . However, in the time series measured before the addition of ATP, we observe only up to two open channels at the same time, which suggests  $\ell = 2$ . This can be explained by the strongly competitive gating suggested by the estimated parameters. In fact, the left upper corner part of the transition matrix  $Q^{(\text{VND})}$  of the hidden Markov chain within the VND model for  $\ell$  channels, which can be estimated from the data at hand, takes

the form

$$U^{(\text{VND}, \ell)} := \begin{pmatrix} \lambda_0^\ell & \ell \lambda_0^{\ell-1}(1 - \lambda_0) & \frac{\ell(\ell-1)}{2} \lambda_0^{\ell-2}(1 - \lambda_0)^2 \\ \lambda_1^{\ell-1}(1 - \eta_1) & q_{1,1} & q_{1,2} \\ \lambda_1^{\ell-2}(1 - \eta_2)^2 & q_{2,1} & q_{2,2} \end{pmatrix}$$

with

$$\begin{aligned} q_{1,1} &:= \lambda_1^{\ell-1} \eta_1 + (\ell - 1) \lambda_1^{\ell-2} (1 - \lambda_1) (1 - \eta_1) \\ q_{1,2} &:= (\ell - 1) \lambda_1^{\ell-2} (1 - \lambda_1) \eta_1 + \frac{(\ell - 1)(\ell - 2)}{2} \lambda_1^{\ell-3} (1 - \lambda_1) (1 - \eta_1)^2 \\ q_{2,1} &:= 2 \lambda_2^{\ell-2} \eta_2 (1 - \eta_2) + (\ell - 2) \lambda_2^{\ell-3} (1 - \lambda_2) (1 - \eta_2)^2 \\ q_{2,2} &:= \lambda_2^{\ell-2} \eta_2^2 + 2(\ell - 2) \lambda_2^{\ell-3} (1 - \lambda_2) \eta_2 (1 - \eta_2) \\ &\quad + \frac{(\ell - 2)(\ell - 3)}{2} \lambda_2^{\ell-4} (1 - \lambda_2)^2 (1 - \eta_2)^2. \end{aligned}$$

This shows that determining  $\ell$  from the data is very difficult since the entries of  $U^{(\text{VND}, \ell)}$  depend only very weakly on  $\ell$  (in analogy of estimating the number of trials within a binomial distribution with small success probability).

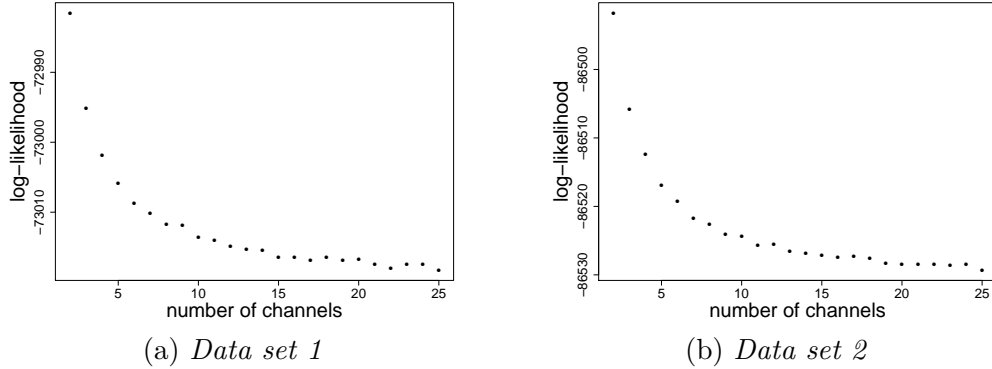


Figure 7: *Log-likelihood estimates of the VND model for  $\ell \in \{2, \dots, 25\}$ . For both data sets, the log-likelihood decreases with the number of channels, which indicates that  $\ell = 2$  provides the best fit.*

As we can see in Figure 7 the dependence on the number of channels is rather weak. It turns out that a model with  $\ell = 2$  appears to provide the best fit. However, this result hinges on the matrix entries  $q_{0,2}$  and  $q_{2,0}$ , which differ most clearly between estimated matrices for different  $\ell$ , both increasing with  $\ell$ . Both entries are very small and could be distorted due to signal filtering in the experiment. Therefore, the results remain inconclusive apart from the finding that the parameter  $\ell$  is very difficult to identify from the present data set.

## References

- Ball, F., R. K. Milne, I. D. Tame, and G. F. Yeo (1997). Superposition of interacting aggregated continuous-time Markov chains. *Adv. Appl. Probab.* 29(1), 56–91.
- Ball, F. G. and J. A. Rice (1992). Stochastic models for ion channels: Introduction and bibliography. *Math. Biosci.* 112(2), 189–206.
- Baum, L. E. and T. Petrie (1966). Statistical inference for probabilistic functions of finite state Markov chains. *Ann. Math. Stat.* 37(6), 1554–1563.
- Baum, L. E., T. Petrie, G. Soules, and N. Weiss (1970). A maximization technique occurring in the statistical analysis of probabilistic functions of Markov chains. *Ann. Math. Stat.* 41(1), 164–171.
- Becker, J. D., J. Honerkamp, J. Hirsch, U. Fröbe, E. Schlatter, and R. Greger (1994). Analysing ion channels with hidden Markov models. *Pflügers Arch.* 426(3), 328–332.
- Bielecki, T., J. Jakubowski, and M. Nieweglowski (2013). Intricacies of dependence between components of multivariate markov chains: weak markov consistency and weak markov copulae. *Electron. J. Probab.* 18, 21 pp.
- Brand, M., N. Oliver, and A. Pentland (1997). Coupled hidden Markov models for complex action recognition. In *Proc. IEEE Comput. Soc. Conf. Comput. Vis. Pattern Recognit.*, pp. 994–999.
- Cappé, O., E. Moulines, and T. Ryden (2005). *Inference in Hidden Markov Models*. Springer Series in Statistics. New York: Springer-Verlag.
- Chen, C., J. Liang, H. Zhao, H. Hu, and J. Tian (2009). Factorial HMM and parallel HMM for gait recognition. *IEEE T. Syst. Man. Cy. C* 39(1), 114–123.
- Chen, W., J. A. Wasserstrom, and Y. Shiferaw (2009). Role of coupled gating between cardiac ryanodine receptors in the genesis of triggered arrhythmias. *Am. J. Physiol. Heart Circ. Physiol.* 297(1), H171–180.
- Chen, Y., K. Shen, S.-O. Shan, and S. C. Kou (2016). Analyzing single-molecule protein transportation experiments via hierarchical hidden Markov models. *J. Am. Stat. Assoc.* 111(515), 951–966.
- Chung, S.-H., O. S. Anderson, and V. V. Krishnamurthy (Eds.) (2007). *Biological Membrane Ion Channels: Dynamics, Structure, and Applications*. Biological and Medical Physics, Biomedical Engineering. New York: Springer-Verlag.
- Chung, S.-H. and R. A. Kennedy (1996). Coupled Markov chain model: Characterization of membrane channel currents with multiple conductance sublevels as partially coupled elementary pores. *Math. Biosci.* 133(2), 111–137.

- Dabrowski, A. R. and D. McDonald (1992). Statistical analysis of multiple ion channel data. *Ann. Stat.* 20(3), 1180–1202.
- de Gunst, M. C. M., H. R. Kunsch, and J. G. Schouten (2001). Statistical analysis of ion channel data using hidden markov models with correlated state-dependent noise and filtering. *J. Am. Stat. Assoc.* 96(455), 805–815.
- Diehn, M., A. Munk, and D. Rudolf (2019). Maximum likelihood estimation in hidden Markov models with inhomogeneous noise. *ESAIM Probab. Stat.* 23, 492–523.
- Fine, S., Y. Singer, and N. Tishby (1998). The hierarchical hidden Markov model: Analysis and applications. *Mach. Learn.* 32(1), 41–62.
- Fredkin, D. R. and J. A. Rice (1991). On the superposition of currents from ion channels. *Philos. Trans. R. Soc. Lond., B, Biol. Sci.* 334(1271), 347–356.
- Ghahramani, Z. and M. I. Jordan (1997). Factorial hidden Markov models. *Mach. Learn.* 29(2), 245–273.
- Gnanasambandam, R., M. S. Nielsen, C. Nicolai, F. Sachs, J. P. Hofgaard, and J. K. Dreyer (2017). Unsupervised idealization of ion channel recordings by minimum description length: Application to human PIEZO1-channels. *Front. Neuroinform.* 11.
- Gottschau, A. (1992). Exchangeability in multivariate Markov chain models. *Biometrics* 48(3), 751–763.
- Guan, X., R. Raich, and W.-K. Wong (2016). Efficient multi-instance learning for activity recognition from time series data using an auto-regressive hidden Markov model. In *Proceedings of the 33rd International Conference on Machine Learning - Volume 48*, ICML’16, New York, NY, USA, pp. 2330–2339. JMLR.org.
- Keleshian, A. M., R. O. Edeson, G.-J. Liu, and B. W. Madsen (2000). Evidence for cooperativity between nicotinic acetylcholine receptors in patch clamp records. *Biophys. J.* 78(1), 1–12.
- Kemeny, J. G. and J. L. Snell (1976). *Finite Markov chains: With a new appendix "generalization of a fundamental matrix"*. Undergraduate Texts in Mathematics. New York: Springer-Verlag.
- Khan, R. N., B. Martinac, B. W. Madsen, R. K. Milne, G. F. Yeo, and R. O. Edeson (2005). Hidden Markov analysis of mechanosensitive ion channel gating. *Math. Biosci.* 193(2), 139–158.
- Klein, S., J. Timmer, and J. Honerkamp (1997). Analysis of multichannel patch clamp recordings by hidden Markov models. *Biometrics* 53(3), 870–884.



- Krogh, A., B. Larsson, G. von Heijne, and E. L. L. Sonnhammer (2001). Predicting transmembrane protein topology with a hidden markov model: Application to complete genomes. *J. Mol. Biol.* 305(3), 567–580.
- Laver, D. R., E. R. O’Neill, and G. D. Lamb (2004). Luminal  $\text{Ca}^{2+}$ -regulated  $\text{Mg}^{2+}$  inhibition of skeletal RyRs reconstituted as isolated channels or coupled clusters. *J. Gen. Physiol.* 124(6), 741–758.
- Manogaran, G., V. Vijayakumar, R. Varatharajan, P. Malarvizhi Kumar, R. Sundarasekar, and C.-H. Hsu (2018). Machine learning based big data processing framework for cancer diagnosis using hidden Markov model and GM clustering. *Wireless. Pers. Commun.* 102(3), 2099–2116.
- Mari, J.-F., J.-P. Haton, and A. Kriouile (1997). Automatic word recognition based on second-order hidden Markov models. *IEEE T. Audio Speech* 5(1), 22–25.
- Marx, S. O., J. Gaburjaková, M. Gaburjakova, C. A. Henrikson, K. Ondrias, and A. R. Marks (2001). Coupled gating between cardiac calcium release channels (ryanodine receptors). *Circ. Res.*
- Meli, A., M. M. Refaat, M. Dura, S. Reiken, A. Wronska, J. Wojciak, J. Carroll, M. M. Scheinman, and A. R. Marks (2011). A novel ryanodine receptor mutation linked to sudden death increases sensitivity to cytosolic calcium. *Circ. Res.*
- Mirams, G. R., Y. Cui, A. Sher, M. Fink, J. Cooper, B. M. Heath, N. C. McMahon, D. J. Gavaghan, and D. Noble (2011). Simulation of multiple ion channel block provides improved early prediction of compounds’ clinical torsadogenic risk. *Cardiovasc. Res* 91(1), 53–61.
- Neukirch, M., D. Rudolf, X. Garcia, and S. Galiana (2019). Amplitude-phase decomposition of the magnetotelluric impedance tensor. *Geophysics* 84(5), E301–E310.
- Pein, F., I. Tecuapetla-Gomez, O. M. Schütte, C. Steinem, and A. Munk (2018). Fully automatic multiresolution idealization for filtered ion channel recordings: Flickering event detection. *IEEE Trans. Nanobioscience* 17, 300–320.
- Perkel, J. M. (2010). High-throughput ion channel screening: A “patch”-work solution. *Biotechniques* 48(1), 25–29.
- Sakmann, B. and E. Neher (Eds.) (1995). *Single-channel recording* (Second ed.). Springer US.
- Salvage, S. C., E. M. Gallant, N. A. Beard, S. Ahmad, H. Valli, J. A. Fraser, C. L.-H. Huang, and A. F. Dulhunty (2019). Ion channel gating in cardiac ryanodine receptors from the arrhythmic RyR2-P2328S mouse. *J. Cell Sci.* 132(10).

- Sherlock, C., T. Xifara, S. Telfer, and M. Begon (2013). A coupled hidden markov model for disease interactions. *J. R. Stat. Soc. C-Appl.* 62(4), 609–627.
- Siekman, I., M. Fackrell, E. J. Crampin, and P. Taylor (2016). Modelling modal gating of ion channels with hierarchical markov models. *Proc. R. Soc. A.* 472.
- Sin, B. and J. H. Kim (1995). Nonstationary hidden Markov model. *Signal Process.* 46(1), 31–46.
- Staudt, T., T. Aspelmeier, O. Laitenberger, C. Geisler, A. Egner, and A. Munk (2020). Statistical molecule mounting in super-resolution fluorescence microscopy: Towards quantitative nanoscopy. *Stat. Sci.* 35(1), 92–111.
- Taur, Y. and W. Frishman (2005). The cardiac ryanodine receptor (RyR2) and its role in heart disease. *Cardiol. Rev.* 13(3), 142–146.
- Touloupou, P., B. Finkenstädt, and S. E. F. Spencer (2020). Scalable bayesian inference for coupled hidden markov and semi-markov models. *J. Comput. Graph. Stat.* 29(2), 238–249.
- van der Kamp, W. S. and N. D. Osgood (2017). Multivariate hidden markov models for personal smartphone sensor data: time series analysis. In *2017 IEEE Int. Conf. Healthc. Inform.*, pp. 179–188.
- Venkataramanan, L. and F. J. Sigworth (2002). Applying hidden Markov models to the analysis of single ion channel activity. *Biophys. J.* 82(4), 1930–1942.
- Walker, M. A., T. Kohl, S. E. Lehnart, J. L. Greenstein, W. J. Lederer, and R. L. Winslow (2015). On the adjacency matrix of ryr2 cluster structures. *PLOS Computational Biology* 11(11), 1–21.
- Walker, M. A., G. S. B. Williams, T. Kohl, S. E. Lehnart, M. S. Jafri, J. L. Greenstein, W. J. Lederer, and R. L. Winslow (2014). Superresolution modeling of calcium release in the heart. *Biophys. J.* 107(12), 3018–3029.
- Westhead, D. R. and M. Vijayabaskar (2017). *Hidden Markov models: Methods and protocols*. Springer.
- Williams, A. J., N. L. Thomas, and C. H. George (2018). The ryanodine receptor: Advances in structure and organization. *Current Opinion in Physiology* 1, 1–6.
- Yeo, G. F., R. O. Edeson, R. K. Milne, and B. W. Madsen (1989). Superposition properties of independent ion channels. *Proc. R. Soc. Lond., B, Biol. Sci.* 238(1291), 155–170.
- Zucchini, W., I. L. MacDonald, and R. Langrock (2017). *Hidden Markov models for time series: An introduction using R*. CRC press.